I. THE FINGERING PROBLEM IN FLOW THROUGH POROUS MEDIA

II. THE KINETIC EQUATION FOR HAMILTONIAN SYSTEMS

Thesis by

John Weidman McLean

In Partial Fulfillment of the Requirements
for the Degree of
Doctor of Philosophy

California Institute of Technology
Pasadena, California
1980
(Submitted April 11, 1980)

ACKNOWLEDGEMENTS

I wish to thank my advisor, Professor P. G. Saffman, for suggesting the topic of this thesis and for his invaluable help and patience during its development. I am grateful to the faculty, staff, and fellow graduate students of the Applied Math department for many interesting discussions.

My research at Caltech was possible due to the financial support of the Institute and the Department of Energy. The numerical computations were possible thanks to a generous allowance of computer time by the Control Data Corporation.

Finally, I wish to thank Suzanne for her continuing encouragement and support.

ABSTRACT

Part I

The interface between two fluids in a porous media is stable or unstable depending on the densities and viscosities of the fluids. Unstable flows tend to develop into long "fingers" of fluids. Saffman and Taylor (1958) analyzed the two-dimensional steady state shape of a finger neglecting interfacial tension. They found that the solutions to the equations of motion are not unique: the width of the finger is arbitrary.

In this paper, the problem is formulated including the effects of surface tension at the interface. The equations of motion are reduced to a pair of nonlinear integro-differential equations for the shape of the finger. The equations are solved numerically and analyzed by perturbation methods.

The numerical results indicate that the system of equations has a unique solution for nonzero surface tension. Solutions are computed for a wide range of physical parameters. The computed profiles agree well with experimental observations.

The perturbation analysis yields contradictory results. A formal expansion in the surface tension parameter can be obtained for arbitrary finger widths, suggesting that the equations do not have a unique solution. The conflict between the numerics and the perturbations is discussed but not resolved.

The stability of the steady fingers to small disturbances is discussed. Linearized stability analysis indicates the two-dimensional fingers are unstable, a result which is at variance with experiment. The stability analysis of the plane interface reveals some new steady profiles. These profiles are computed for finite amplitude.

Part II

The kinetic equation describing weak nonlinear interactions between wave components in a Hamiltonian system is obtained by perturbation methods. The analysis is facilitated by the use of Wyld diagrams. The results include some new terms not included in previous work. The inconsistency of some previous investigations is pointed out, and the significance of the new terms is discussed.

TABLE OF CONTENTS

ACKNOWLEDGEMENTS ii

ABSTRACT iii

TABLE OF CONTENTS v

I. THE FINGERING PROBLEM IN FLOW THROUGH POROUS MEDIA 1

1. Introduction 2
2. Formulation of the Problem 5
3. Analysis of the Equations 15
4. Numerical Treatment 19
5. Perturbation Solution 31
6. The Conflict Between Numerics and Perturbations 41
7. Linearized Stability Analysis 48
8. Other Steady Solutions 64
9. Discussion 72

APPENDIX A 74

APPENDIX B 77

APPENDIX C 80

APPENDIX D 84

REFERENCES 87

II. THE KINETIC EQUATION FOR HAMILTONIAN SYSTEMS 88

1. Introduction 89
2. Formulation of the Problem 92
3. The Perturbation Expansion 98
4. Analysis of the Diagrams 109
5. Discussion 117

REFERENCES 119

Part I

THE FINGERING PROBLEM IN FLOW THROUGH POROUS MEDIA

1. INTRODUCTION

It is well-known that when two superposed fluids of different densities are accelerated in a direction perpendicular to the surface, the interface will be unstable if the acceleration is from the less dense fluid to the more dense fluid (Taylor 1950). A similar instability may occur in a porous medium where a less viscous fluid drives a more viscous fluid (Saffman and Taylor 1958). This instability is responsible for water flooding of oil wells, and is of considerable importance to oil reservoir engineering (Wooding and Morel-Seytoux 1976).

In order to study this instability, experiments have been performed in a Hele-Shaw cell: a channel formed by two closely spaced, parallel glass plates (Saffman and Taylor 1958, Pitts 1980). It was observed that the unstable interface forms into a number of "fingers." After a sufficient time, the flow reaches the steady state of a single finger propagating without change of shape (Fig. 1-1). Our interest will be in the steady-state shape of these fingers.

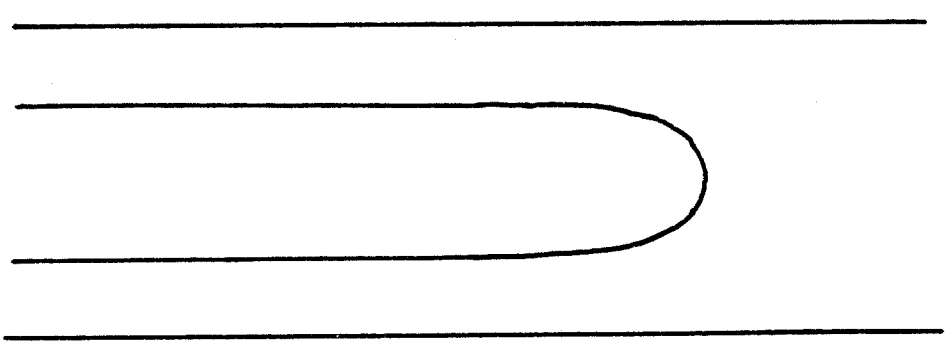

Figure 1-1

The shape of these fingers has been obtained mathematically by neglecting surface tension effects at the interface (Saffman and Taylor 1958). Surprisingly, the solution was obtained in closed form. The solution, however, was not determined uniquely. The width of the finger, λ, enters into the solution as an arbitrary parameter. In experiments where the surface tension is small, λ is close to one-half. Comparisons of the experimental shapes with the Saffman-Taylor solution for $\lambda = 1/2$ yields excellent agreement.

As the surface tension becomes important, the width of the finger increases to fill the channel. The Saffman-Taylor solution deviates from the experimental shapes for finite surface tension.

Several attempts have been made to remove the ambiguity in the Saffman-Taylor result. In a recent article, Pitts (1980) uses some heuristic arguments about the nature of the motion at the interface to obtain an equation for the finger shapes. His results remove the nonuniqueness of the Saffman-Taylor solution. His formula agrees well with a wide range of experiments, but deviates for large surface tension.

In this presentation, the effects of surface tension are included at the interface. The equations of motion are derived. The equations for the shape of the free surface are reduced to a pair of coupled, nonlinear, integro-differential equations.

For finite surface tension, the equations for the free surface are replaced by a finite difference form and solved numerically using Newton's method. The numerical scheme converged quadratically in

all cases. Due to the behavior of the numerics, it is proposed that the equations for the free surface have a unique solution for nonzero surface tension. The numerical profiles are compared with experimental photographs, and in all cases show excellent agreement.

The case of small surface tension is examined by perturbation methods. A regular perturbation expansion is carried out to three terms. Although the expansion is nonuniform at one endpoint, the "outer" expansion can be matched to the local expansion. The perturbation solution can be formally constructed for arbitrary finger widths, suggesting that the equations for the free surface do not have a unique solution.

The apparent contradiction between the numerical solution and the perturbation expansion is discussed but not resolved.

Stability of the plane interface is examined. For small surface tension, the plane interface is unstable, a result first obtained by Saffman and Taylor. The stability of the steady fingers is investigated. The mathematical result of Saffman and Taylor indicates that the fingers are unstable when surface tension is neglected. We have included surface tension in the analysis, but the results indicate the finger is still unstable to disturbances. This result does not agree with experimental observations.

The stability analysis of the plane interface indicates other steady solutions are possible. These solutions are obtained by perturbation methods and computed numerically to finite amplitude.

2. FORMULATION OF THE PROBLEM

We consider two-dimensional, incompressible flow in a porous medium. The flow of fluids in a porous media is governed by Darcy's law (Darcy 1856):

$$\vec{u} = -\frac{k}{\mu}\nabla(p + \rho g x) = \nabla\phi \tag{2-1}$$

where $\vec{u}$ is the velocity vector, μ the viscosity, ρ the density of the fluid, k is the permeability of the medium, and g is the acceleration of gravity. The quantity ϕ is called the velocity potential. Since the fluid is incompressible, continuity yields:

$$\nabla \cdot \vec{u} = \nabla^2\phi = 0 \tag{2-2}$$

Thus, we are interested in potential flow: Laplace's equation appended by some appropriate boundary conditions.

Two-dimensional potential flow can be studied experimentally by means of an analogue developed by Hele-Shaw (Hele-Shaw 1898). The motion of an incompressible viscous fluid between two fixed, closely spaced parallel plates is such that the components of the mean velocity (averaged across the gap) satisfy:

$$u = -\frac{b^2}{12\mu}\left(\frac{\partial p}{\partial x} + \rho g\right) = \phi_x$$

$$v = -\frac{b^2}{12\mu}\left(\frac{\partial p}{\partial y}\right) = \phi_y \tag{2-3}$$

where b is the spacing between the plates (see Lamb 1932, §330). Comparison with (2-1) shows that the motion in a Hele-Shaw cell is equivalent to two-dimensional flow in a porous medium of permeability $b^2/12$.

The experiments reported in the literature (Saffman and Taylor 1958, Pitts 1980) have been performed with the Hele-Shaw cell in a horizontal plane. In this configuration, we assume that gravity has no effect on the mean flow.

Consider the motion of a single finger of fluid penetrating into a more viscous fluid in a Hele-Shaw cell of width a and gap spacing b. The finger moves with velocity U and has width λa.

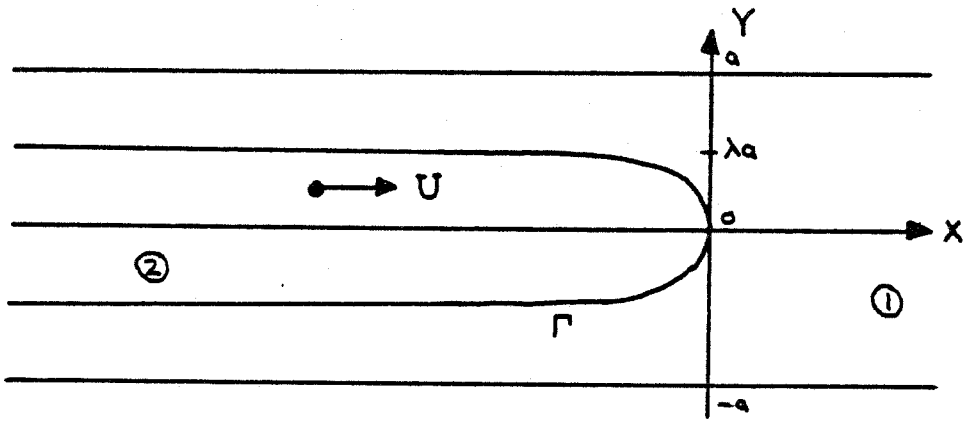

Figure 2-1

Let the suffix ① indicate the more viscous fluid ahead of the finger, suffix ② will denote the fluid in the finger. The velocity satisfies:

$$\vec{u}_1 = \nabla\phi_1 = -\frac{b^2}{12\mu_1}\nabla p_1$$

$$\vec{u}_2 = \nabla\phi_2 = -\frac{b^2}{12\mu_2}\nabla p_2 \qquad (2\text{-}4)$$

At the interface between the fluids there is a kinematic and a dynamic boundary condition. The pressure jump across the interface is balanced by surface tension. The normal component of velocity must be continuous. Thus, on the free surface Γ we have:

$$p_2 - p_1 = T(2/b + 1/R)$$

$$\psi = Uy \tag{2-5}$$

where R is the radius of curvature, ψ is the stream function, and T is the surface tension.

Upstream, fluid (1) moves with uniform velocity $V = \lambda U$. Inside the finger, the fluid simply translates. The walls of the Hele-Shaw cell are streamlines. Thus, we look for an analytic function $w_1(x, y)$ which satisfies:

$$\begin{aligned} w_1 &= \phi_1 + i\psi_1 \\ \psi_1 &= \pm Va && \text{on } y = \pm a \\ \phi_1 &= \left(\frac{Tb^2}{12\mu_1}\right)\frac{1}{R} + \left(\frac{\mu_2}{\mu_1}\right)\phi_2 \\ \psi_1 &= Uy \end{aligned} \Bigg\} \quad \text{on } \Gamma$$

$$\phi_1 \sim \lambda Ux \qquad \text{as } x \to +\infty \tag{2-6}$$

For $T = 0$, $\mu_2 = 0$, the flow region in the potential plane is a semi-infinite strip, with given boundary values on the edges. A solution in closed form has been obtained (Saffman and Taylor 1958):

$$x_0 = \frac{(1-\lambda)a}{\pi} \ell n \frac{1}{2}\left(1 + \cos\frac{\pi y}{\lambda a}\right) + Ut \tag{2-7}$$

The solution for nonzero μ_2 can be obtained by scaling the velocities, but the shape is still given by (2-7).

The parameter λ is undetermined by the analysis for $T = 0$. Experiments performed with fluids having small interfacial tension give values of λ close to one-half. Comparison of the experimental profiles with (2-7) evaluated with $\lambda = 1/2$ yields excellent agreement. Experiments where the interfacial tension is significant have values of λ greater than one-half. In these experiments, (2-7) deviates from the measured profiles.

Pitts (1980) examined the motion in the vicinity of the interface in an attempt to determine the parameter λ. Based on experimental observations, he formulated a model of the flow. The subsequent analysis determines λ as a function of $\mu U/T$, and the profiles are given by:

$$x = \frac{\lambda a}{\pi} \log \frac{1}{2}\left(1 + \cos \frac{\pi y}{\lambda a}\right) + Ut \qquad (2\text{-}8)$$

The Saffman-Taylor solution (2-7) and the Pitts solution (2-8) are plotted against experimental results in figures 4-2, 4-3, and 4-4. Although Pitts' solution yields better comparison with experiment, the derivation of (2-8) cannot be considered rigorous.

Our analysis will be based on the hydrodynamic equations (2-6). For nonzero surface tension, the flow in the potential plane is no longer a strip. In a frame of reference moving with the finger, however, the potential plane again is simple.

$$u_{moving} = u_{fixed} - U$$

$$\phi_{moving} = \phi_{fixed} - Ux$$

The variables are scaled to make the problem dimensionless:

$$\hat{y} = y/a \qquad \hat{x} = (x - Ut)/a$$

$$\hat{\psi} = \frac{\psi_{moving}}{(1-\lambda)\,Ua} \qquad \hat{\phi} = \frac{\phi_{moving}}{(1-\lambda)\,Ua}$$

$$\frac{1}{R} = \frac{-\,d^2x/dy^2}{\left[1 + \left(\frac{dx}{dy}\right)^2\right]^{3/2}} = -\frac{1}{a}\,\frac{d^2\hat{x}/d\hat{y}^2}{\left[1 + \left(\frac{d\hat{x}}{d\hat{y}}\right)^2\right]^{3/2}} \qquad (2\text{-}9)$$

$$= \frac{1}{a}\,\frac{1}{\hat{R}}$$

Since we expect the fingers to be symmetric, we consider half of the finger. In a coordinate system moving with the finger, the interface will be a streamline. Dropping ($\hat{}$), the flow is as follows:

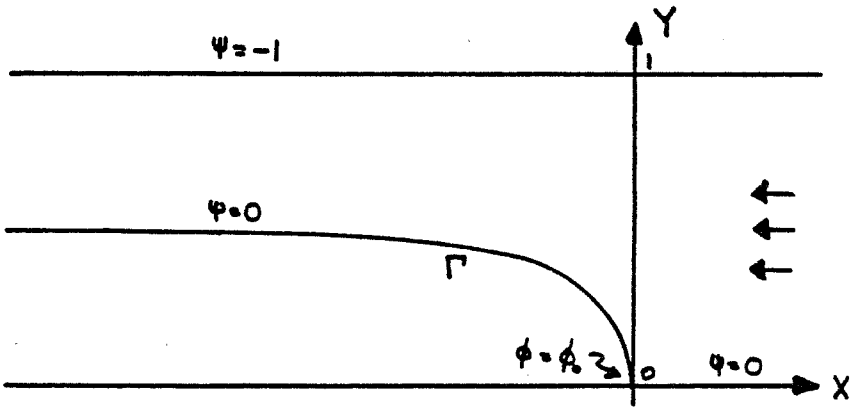

Figure 2-2

The equations (2-6) became (dropping $\hat{}$):

$$w = \phi + i\psi \quad \text{analytic} \tag{2-10a}$$

$$\psi = -1 \qquad \text{on } y = 1 \tag{2-10b}$$

$$\left.\begin{aligned} \phi &= \left(\frac{T}{12\mu U}\right)\left(\frac{b}{a}\right)^2 \frac{1}{1-\lambda}\left(\frac{1}{R} - \frac{x}{1-\lambda}\right) \\ \psi &= 0 \end{aligned}\right\} \quad \text{on } \Gamma \tag{2-10c, 2-10d}$$

$$\phi \sim -x \qquad \text{as } x \to +\infty \tag{2-10e}$$

Since the flow in this frame of reference is bounded by streamlines, the flow in the potential plane will have a simple geometry.

In Cartesian coordinates, the radius of curvature which appears in the boundary condition is a complicated function of derivatives of x and y. To simplify this term, we work with the magnitude of the velocity q, and the flow angle θ (Crapper 1957).

$$qe^{i\theta} = u + iv$$

$$u = q\cos\theta \tag{2-11}$$

$$v = q\sin\theta$$

If s measures arclength along the interface, the radius of curvature is:

$$\frac{1}{R} = \frac{d\theta}{ds} = \left(\frac{\partial\theta}{\partial\phi}\right)\frac{d\phi}{ds} = q\left(\frac{\partial\theta}{\partial\phi}\right)\Big|_{\psi = 0} \tag{2-12}$$

Since:

$$\frac{dz}{dw} = \frac{1}{q} e^{i\theta} = \frac{\partial x}{\partial \phi} + i \frac{\partial y}{\partial \phi}$$

$$\log\left(\frac{dz}{dw}\right) = -\log q + i\theta \qquad (2\text{-}13)$$

Then $-\log q$ and θ are conjugate harmonic functions. Integrating (2-13) along the interface ($\psi = 0$) gives a parametric representation of the finger:

$$x(\phi) = \int_{\phi_0}^{\phi} \frac{\cos\theta}{q}\, d\phi$$

$$y(\phi) = \int_{\phi_0}^{\phi} \frac{\sin\theta}{q}\, d\phi \qquad (2\text{-}14)$$

The flow picture is:

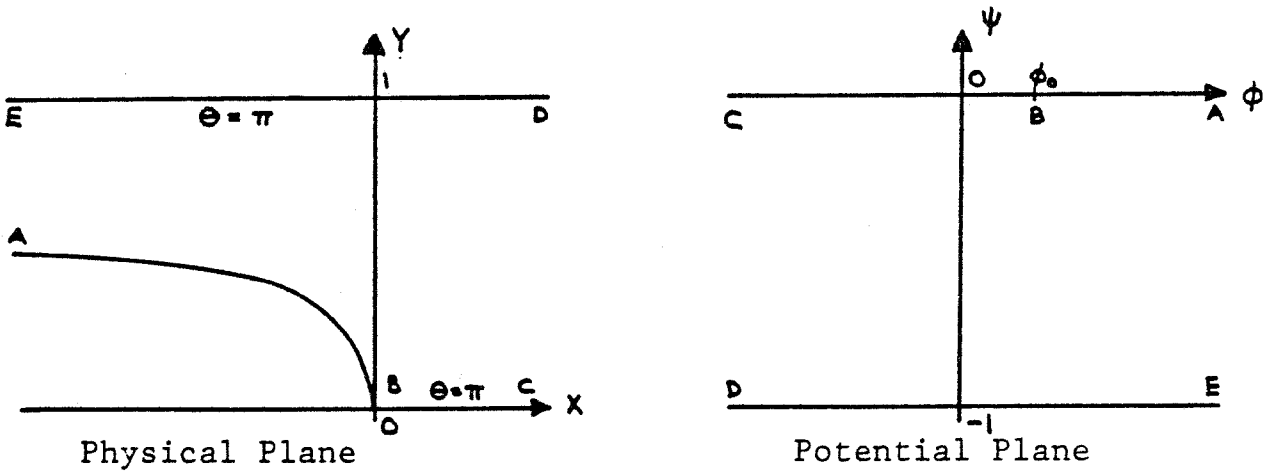

Figure 2-3

On the interface AB, the nonlinear boundary condition (2-10c) is applied.

A conformal mapping is used to map the strip $-1 < \psi < 0$ onto the upper half plane:

$$W = e^{-(w-\phi_0)\pi} = s + it \tag{2-15}$$

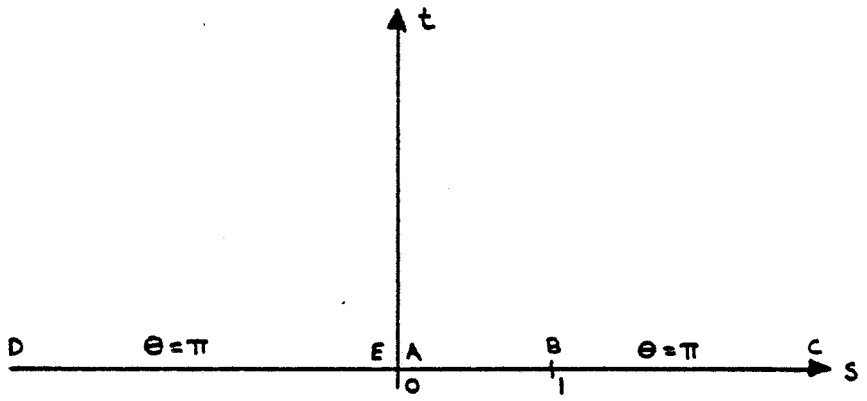

Figure 2-4

Using Cauchy's integral formula, we can relate $-\log q$ to θ along the boundary. We have:

$$\log q = -\frac{1}{\pi} \mathrm{P}\int_0^1 \frac{\theta(s')-\pi}{s'-s}\, ds' \tag{2-16}$$

The integral is interpreted as a Cauchy principal value. The boundary condition (2-10c) becomes:

$$\log s = \left(\frac{T\pi^2}{12\mu U}\right)\left(\frac{b}{a}\right)^2 \frac{1}{1-\lambda}\, s\, q\left(\frac{\partial\theta}{\partial s}\right) - \frac{1}{1-\lambda} \int_1^s \frac{\cos\theta}{qs}\, ds + \pi\phi_0 \tag{2-17}$$

Equations (2-16) and (2-17) constitute two equations for the two unknowns q and θ on $0 < s < 1$. One further scaling simplifies the equations:

$$\tilde{q} = (1-\lambda)q$$

$$\tilde{\theta} = \theta - \pi \qquad (2\text{-}18)$$

The equations become (after differentiating):

$$\tilde{q} = k\tilde{q}s \frac{d}{ds}\left(\tilde{q}s \frac{d\tilde{\theta}}{ds}\right) + \cos\tilde{\theta} \qquad (2\text{-}19a)$$

$$\log \tilde{q} = -\frac{s}{\pi} \fint_0^1 \frac{\tilde{\theta}(s')}{s'(s'-s)}\, ds' \qquad (2\text{-}19b)$$

$$\tilde{\theta}(0) = 0 \quad \tilde{\theta}(1) = -\pi/2$$

$$\tilde{q}(0) = 1 \quad \tilde{q}(1) = 0 \qquad (2\text{-}19c)$$

where

$$k = \frac{T\pi^2}{12\mu U}\left(\frac{b}{a}\right)^2 \left(\frac{1}{1-\lambda}\right)^2$$

$$\log(1-\lambda) = \frac{1}{\pi} \int_0^1 \frac{\tilde{\theta}(s')}{s'}\, ds' \qquad (2\text{-}20)$$

The boundary conditions for $\tilde{q}$ and $\tilde{\theta}$ are given by physical considerations. At the nose of the finger ($s = 1$), there must be a stagnation point and the tangent to the finger must be vertical. At the tail ($s = 0$), the flow is uniform. Note that the boundary conditions on $\tilde{q}$ are consistent with the equations.

These equations are to be solved on $0 < s < 1$. After solving (2-19) for $\tilde{q}$ and $\tilde{\theta}$, the coordinates of the interface are given parametrically

by:

$$x(s) = \frac{1-\lambda}{\pi} \int_1^s \frac{\cos\tilde{\theta}}{\tilde{q}\, s}\, ds$$

$$y(s) = \frac{1-\lambda}{\pi} \int_1^s \frac{\sin\tilde{\theta}}{\tilde{q}\, s}\, ds \qquad (2\text{-}21)$$

Note that since $y(0) = \lambda$, the width of the finger may be computed either from (2-20) or (2-21).

In these variables, the solution by Saffman and Taylor (2-7) is:

$$\tilde{q}_0 = \sqrt{\frac{1-s}{1+s\phi}} \qquad \tilde{\theta}_0 = \cos^{-1}\tilde{q}_0$$

$$\phi = \frac{2\lambda-1}{(1-\lambda)^2} \qquad (2\text{-}22)$$

This solution can be shown to satisfy (2-19) for $k=0$ (see Appendix A).

The solution of (2-19) is known for $k=0$. Our interest will be to solve these equations for $k > 0$, and try to understand the nonunique behavior for $k=0$. The results of our calculations will be compared with experimental data. To simply notation, the ($\sim$) will henceforth be dropped.

3. ANALYSIS OF THE EQUATIONS

There are two goals in the examination of (2-19). First, we wish to calculate the profile of the finger and compute its width for finite values of k. Secondly, the nature of the limiting process $k \to 0$ is to be investigated. For small k, a perturbation approach is attempted. For finite k, (2-19) is solved numerically.

The coefficients of the derivatives in (2-19a) vanish at $s = 0$ and $s = 1$, so we expect singular behavior at the endpoints of the interval. The theory of a regular singular point in ODE's suggest the solution about $s = 0$ is:

$$\theta(s) = s^{\tau} \sum_{0}^{\infty} a_n s^n \tag{3-1}$$

Substitution of this series into (2-19b) leads to terms like $s^{2\tau}$, $s^{3\tau}$ etc., which cannot be matched by (3-1). We therefore look for a solution which begins:

$$\begin{aligned} \theta(s) &= a_1 s^{\tau} + a_2 s^{2\tau} + O\left(s^{3\tau}, s, s^{1+\tau}\right) \\ q(s) &= 1 + b_1 s^{\tau} + b_2 s^{2\tau} + O\left(s^{3\tau}, s, s^{1+\tau}\right). \end{aligned} \tag{3-2}$$

The expansion (3-2) is substituted into (2-19a):

$$1 + b_1 s^{\tau} + b_2 s^{2\tau} + \cdots = k\left(\tau^2 a_1 s^{\tau} + \tau^2 (3a_1 b_1 + 4a_2) s^{2\tau} + \cdots\right) + 1 - \frac{a_1^2}{2} s^{2\tau} + \cdots \tag{3-3}$$

Equating coefficients yields:

$$b_1 = k\tau^2 a_1$$

$$b_2 = k\tau^2(3a_1b_1 + 4a_2) - a_1^2/2 \tag{3-4}$$

$$\vdots$$

For equation (2-19b), we must evaluate the principal value integral. Using the result:

$$\mathcal{P}\int_0^1 \frac{x^\beta}{x-y}\,dx = \frac{1}{\beta} + \frac{y}{\beta-1} - \pi y^\beta \cot \pi\beta + O(y^2) \tag{3-5}$$

$$0 < \beta < 1$$

the expansion of (2-19b) becomes:

$$b_1 s^\tau + \left(b_2 - b_1^2/2\right)s^{2\tau} + \cdots$$

$$= a_1 \cot \pi\tau\, s^\tau + a_2 \cot 2\pi\tau\, s^{2\tau}$$

$$- \frac{1}{\pi}\left(\frac{a_1}{\tau-1} + \frac{a_2}{2\tau-1} + \cdots\right)s + \cdots \tag{3-6}$$

Equating coefficients:

$$b_1 = a_1 \cot \pi\tau$$

$$b_2 - b_1^2/2 = a_2 \cot 2\pi\tau \tag{3-7}$$

$$\vdots$$

Comparing (3-4) and (3-7) we have:

$$\frac{1}{\tau^2}\cot\pi\tau = k \tag{3-8}$$

The coefficients b_1, b_2, and a_2 are determined recursively as functions of a_1. As $k \to 0$, (3-8) shows that $\tau \to 1/2$, which agrees with the Saffman-Taylor solution (2-22).

Since cotangent is periodic, (3-8) has multiple solutions, suggesting that extra powers of s can appear in the expansion (3-2). In particular, for $k=0$: $\tau_n = (2n-1)/2$ are solutions of (3-8) for any integer n. In this case, $\tau_n = (2n-1)\tau_1$, and no new powers of s appear in (3-2). For $k \neq 0$, the exponents $\{\tau_n\}$ are not simple multiples of one another. The expansion (3-2) takes the form:

$$\begin{aligned}\theta(s) = {} & {}_1a_1 s^{\tau_1} + {}_1a_2 s^{2\tau_1} + \cdots \\ & + {}_2a_1 s^{\tau_2} + {}_2a_2 s^{2\tau_2} + \cdots \\ & + \Phi_1 s + \Phi_2 s^2 + \cdots\end{aligned} \tag{3-9}$$

The significance of this change in the local expansion will be explored in Chapter 5.

At the right endpoint ($s = 1$), an expansion of q and θ in powers of $\sqrt{1-s}$ can be shown to be consistent (Appendix B). In this case, the coefficients in the expansion are not determined recursively, but are determined by integrals of θ over the entire interval.

The analysis at the endpoints suggest that the solution is singular like s^{τ} near $s = 0$, and $\sqrt{1-s}$ near $s = 1$. The coefficients in (2-19a) vanish nowhere else, and we expect the solution to be analytic in the interior of the interval.

4. NUMERICAL TREATMENT

We explicitly change independent variables in (2-19) so that q and θ will be differentiable at the endpoints. Let:

$$z = \left(1-s^{\tau}\right)^{1/2} \tag{4-1}$$

The equations (2-19) become (using (3-8)):

$$q = (\cot \pi\tau)\, q\left(\frac{1-z^2}{2z}\right) \frac{d}{dz}\left(q\left(\frac{1-z^2}{2z}\right)\frac{d\theta}{dz}\right) + \cos\theta \tag{4-2a}$$

$$\log q = \frac{1}{\tau\pi}\int_0^1 \left(\frac{2z'}{1-z'^2}\right)\theta(z')dz' - \frac{1}{\tau\pi}\oint_0^1 \left(\frac{2z'}{1-z'^2}\right)\frac{\theta(z')}{1-\left(\frac{1-z^2}{1-z'^2}\right)^{1/\tau}}\,dz' \tag{4-2b}$$

$$\theta(0) = -\pi/2 \qquad \theta(1) = 0$$

$$q(0) = 0 \qquad q(1) = 1 \tag{4-2c}$$

Note that $z = 0$ is the nose of the bubble, while $z = 1$ is the tail.

In these variables, θ and q have at least two derivatives at $z = 1$. The numerics indicate that θ and q are even smoother, and closer examination of the local expansion about $s = 0$ suggests the term linear in s is missing (see Chapter 5). With this term missing, q and θ have three bounded derivatives at $z = 1$.

The integrand in (4-2b) is rewritten to remove the pricipal

value singularity. In this form, the integrand is smooth and may be evaluated numerically.

$$q(z) = \sqrt{1-(1-z^2)^{1/\tau}}\ \exp\left\{-\frac{1}{\tau\pi}\,\mathcal{P}\int_0^1 \left(\frac{2z'}{1-z'^2}\right)\frac{\theta(z')-\theta(z)}{(1-z')^{1/\tau}-(1-z^2)^{1/\tau}}\,(1-z'^2)^{1/\tau}\,dz'\right\}$$

$$\cdot\ \exp\left\{\frac{1}{\tau\pi}\int_0^1 \left(\frac{2z'}{1-z'^2}\right)\theta(z')dz'\right\}$$

$$\cdot\ \exp\left\{\frac{1}{\pi}\,\theta(z)\log(1-z^2)^{1/\tau} - \frac{1}{\pi}\Big(\theta(z)-\theta(0)\Big)\cdot\log\Big(1-(1-z^2)^{1/\tau}\Big)\right\} \qquad (4\text{-}3)$$

By suitable manipulations, the integrand may be made smoother, but comparison of the exact solution (2-22) with the results of numerical integration showed this was not necessary.

A three-point centered difference scheme is used to approximate the derivatives in (4-2a), and the trapezoidal rule is applied to the integral (4-3). The interval [0, 1] is broken into N equal segments of length h = 1/N. We set:

$$\theta_1 \equiv \theta(0) = -\pi/2$$

$$\theta_{N+1} \equiv \theta(1) = 0$$

$$\theta_i \equiv \theta\Big((i-1)\cdot h\Big) \qquad 1 \le i \le N+1$$

We wish to solve for the N-1 unknowns $\{\theta_i\}_{i=2,\ldots,N}$ using the finite difference equations at the N-1 interior mesh points. Newton's method is used to obtain a solution. All computations were performed

on the CDC-STAR 100A vector computer.

Although both the trapezoidal rule and the centered difference quotient are formally accurate to $O(h^2)$, the error term involves fourth derivatives. Since θ and q have only three bounded derivatives at $z = 1$, we must expect loss of accuracy at this endpoint. Comparison of the numerical solution for various mesh spacings indicate that the loss in accuracy is slight, and that the numerical scheme is $O(h^2)$ accurate throughout the interval.

The Newton scheme is said to have converged when the maximum residual at the mesh points is less than 10^{-10}. The accuracy of the CDC machine is close to 13 digits, but the accuracy of the calculations is limited to about 11 digits (for $N = 100$) by roundoff error in the summations for the integrations.

After the Newton scheme has converged, the Cartesian coordinates of the interface are obtained by integration. Using z as an independent variable, the x and y coordinates are given by:

$$x(z) = -\left(\frac{1-\lambda}{\tau\pi}\right) \int_0^z \left(\frac{2z}{1-z^2}\right) \frac{\cos\theta(z)}{q(z)}\, dz$$

$$y(z) = -\left(\frac{1-\lambda}{\tau\pi}\right) \int_0^z \left(\frac{2z}{1-z^2}\right) \frac{\sin\theta(z)}{q(z)}\, dz \qquad (4\text{-}4)$$

The width of the finger is given by:

$$\log(1-\lambda) = \frac{1}{\tau\pi} \int_0^1 \left(\frac{2z}{1-z^2}\right) \theta(z)\, dz \qquad (4\text{-}5)$$

The trapezoidal rule is used to evaluate (4-4) and (4-5). Since $y(1) = \lambda$, the width of the finger may be calculated two different ways. This provides a useful check on the accuracy of the calculations.

Although the equations are known to be singular for $k = 0$ ($\tau = \frac{1}{2}$), it was hoped that the system (2-19) has a unique solution for $k > 0$ ($\tau < \frac{1}{2}$). Using the Saffman-Taylor solution (2-22) evaluated at $\lambda = \frac{1}{2}$ as an initial guess, an attempt was made to compute a solution for $\tau = 0.48$ ($k = 0.273$). Somewhat unexpectedly, the Newton scheme converged quadratically.

To gain confidence in the numerical results, numerous tests have been performed. The number of mesh points N was varied. Solutions have been calculated for 25, 50, 100, and 200 mesh points. The results agree to four decimal places. The initial guess was varied, in all cases converging to the same solution (or diverging if the initial guess was too far away). Since λ is computed two ways, it provides a check on the accuracy of the method. For $N = 100$, the value of λ differed in the fourth decimal place.

We perform continuation in the parameter τ. Using the previous solution as an initial guess, Newton's scheme computes the solution for the next value of τ. Solutions have been obtained for $0.002 < \tau < 0.49$ corresponding to values of k from 0.131 to 4×10^7. For τ very small, large gradients appear in θ and q, and the numerics become unreliable. As τ approaches one-half, the Jacobian becomes singular (Fig. 4-1).

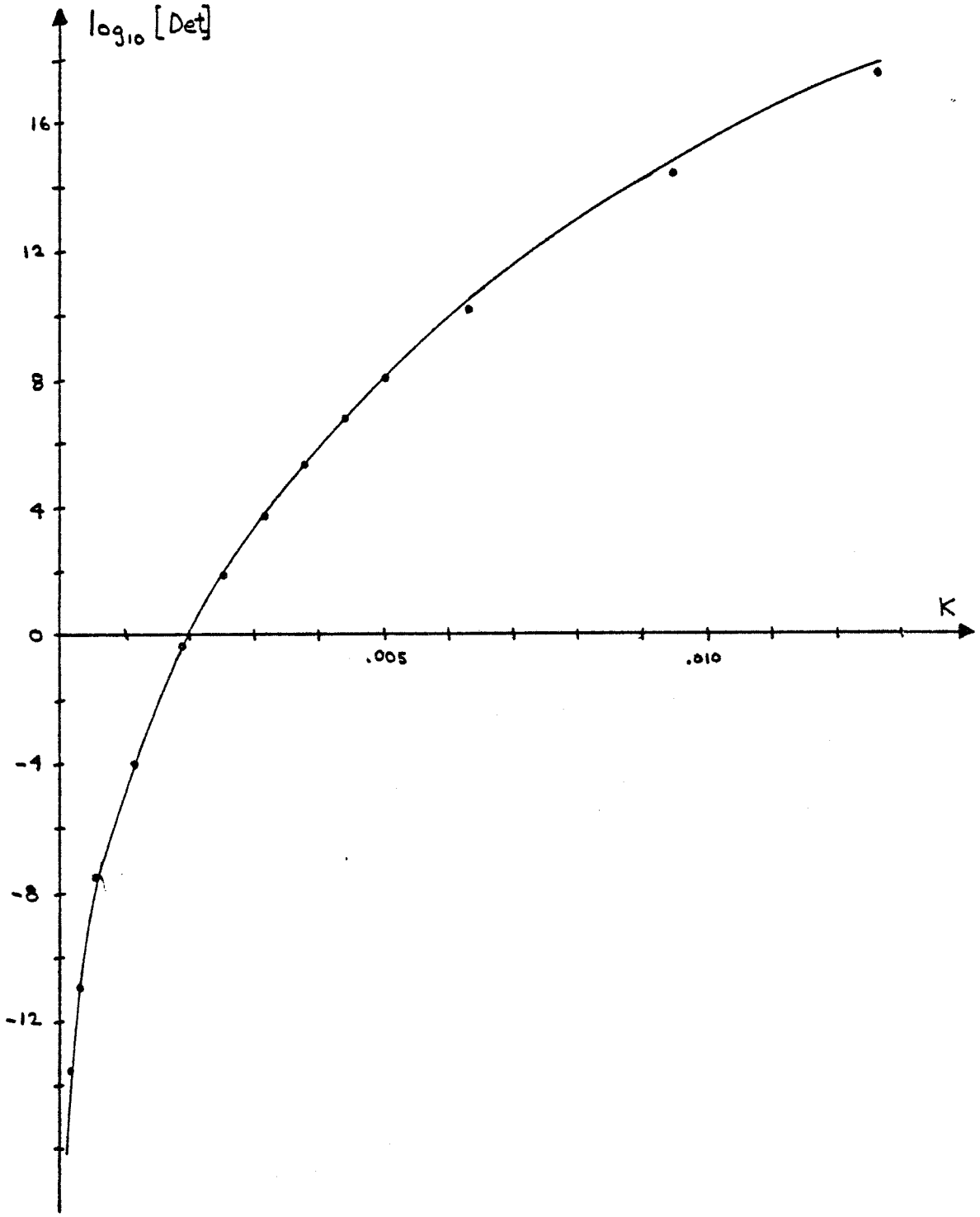

Figure 4-1 Plot of the logarithm of the Jacobian versus the surface tension parameter k (50 mesh points).

The numerical profiles are compared with experimental results in Figures 4-2, 4-3, and 4-4. For a given experimental profile, we plot the numerical solution with the same width. This width is used in the Saffman-Taylor (2-7) and Pitts (2-8) solution for comparison. It should be noted that the fingers photographed by Pitts show a systematic asymmetry, suggesting that the plates in his Hele-Shaw cell might not be exactly parallel.

The relation between the width λ and the parameter k is given in Table 1. The numerical results are plotted against the experimental results of Saffman and Taylor in Figure 4-5. The two curves are displaced.

One possible explansion for this discrepancy is that the analysis leading to (2-19) assumes that the finger completely expels the other fluid from the channel. If we assume that the finger does not fill the channel, but only fills a fraction t of the gap, the flow will be equivalent to a finger which completely expels a fluid of viscosity $t\mu$ (Saffman and Taylor 1958).

Althouth no data are available concerning t in the Hele-Shaw cell, a related experiment has measured the amount of fluid left behind when a viscous fluid is blown from a tube (Taylor 1961). For $0 < \mu U/T < 0.09$, the parameter t in this experiment is given by:

$$t = 1 - (\mu U/T)^{1/2} \qquad (4\text{-}6)$$

For comparison, we have used (4-6) as an approximation for t to correct for the finger not completely filling the gap. As can be

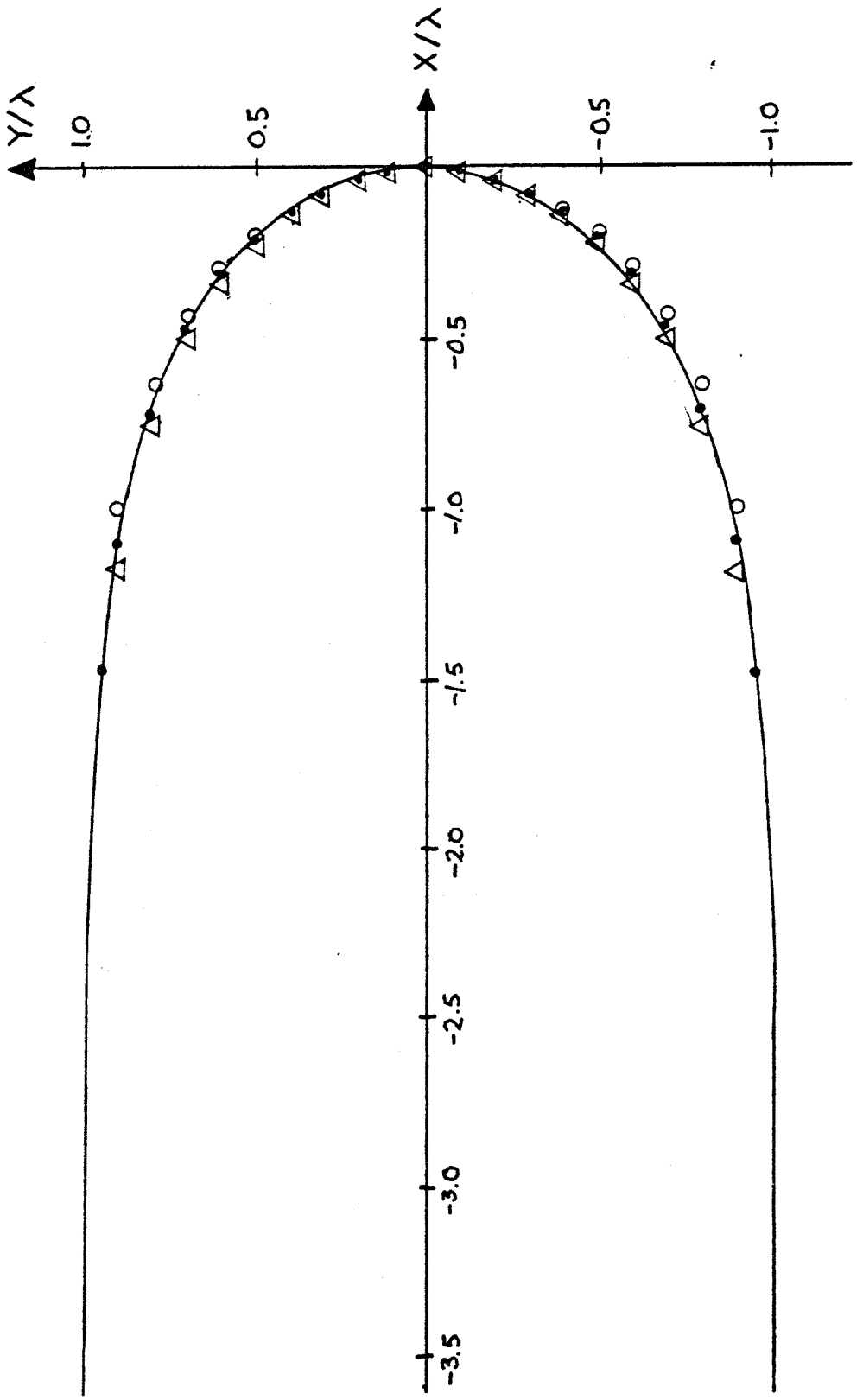

Figure 4-2 Comparison of theory and experiment, λ=0.54. Solid line: experimental profile (Pitts 1980); o Saffman-Taylor solution (2-7); Δ Pitts solution (2-8); • numerical results

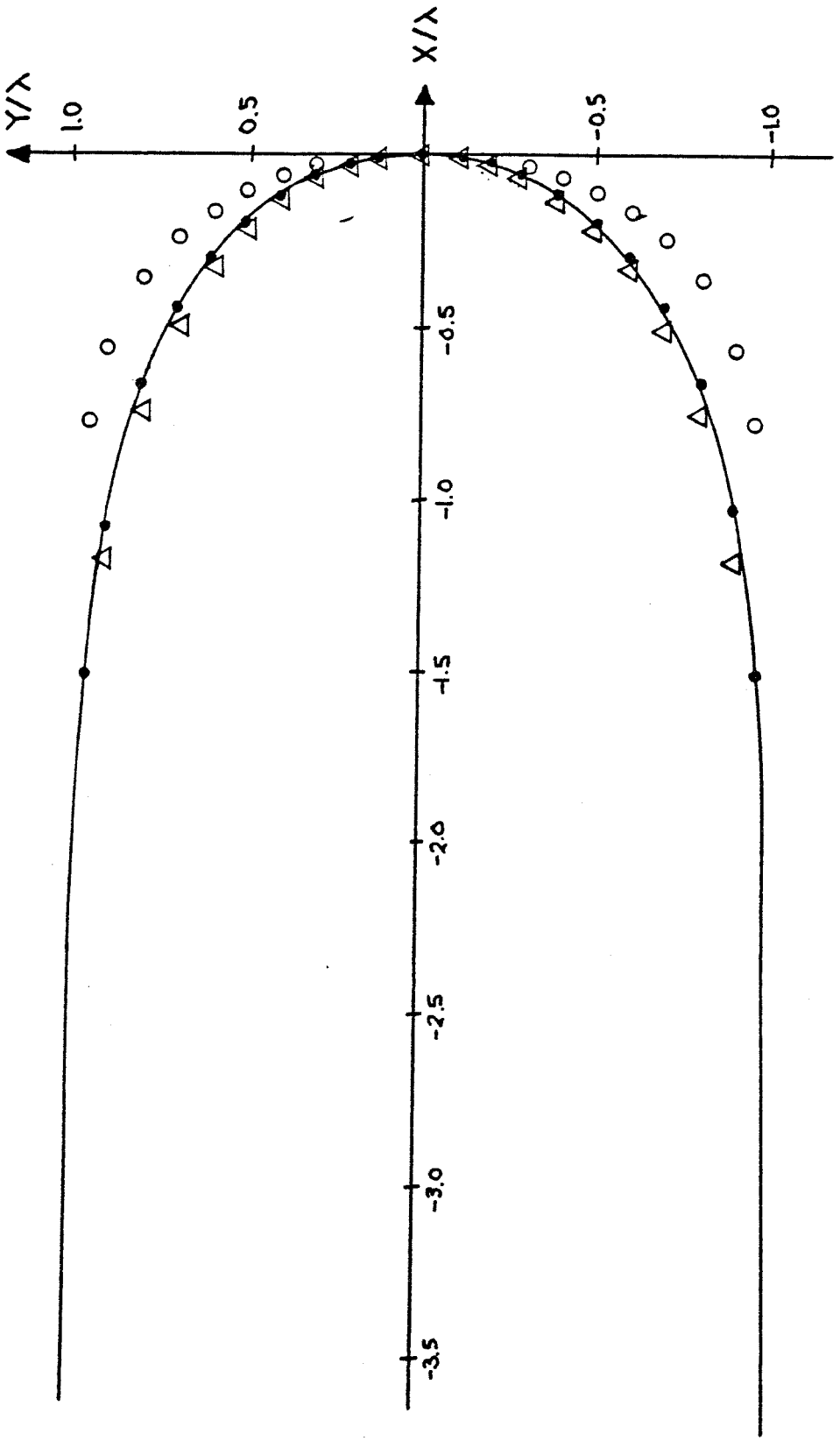

Figure 4-3 Comparison of theory and experiment, λ =0.68. Solid line: experimental profile (Pitts 1980); o Saffman-Taylor solution (2-7); Δ Pitts solution (2-8); • numerical results.

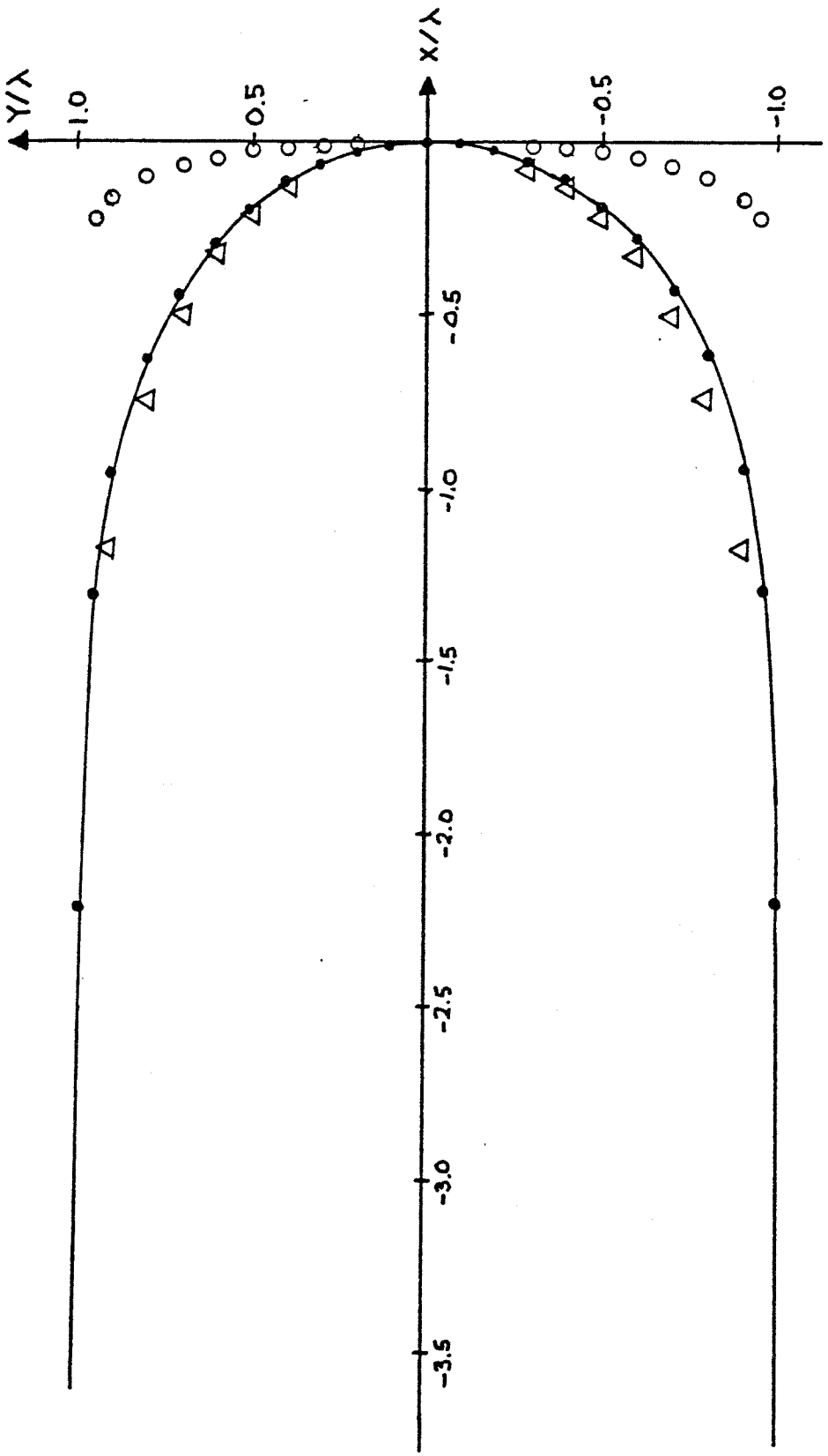

Figure 4-4 Comparison of theory and experiment, $\lambda = 0.88$. Solid line: experimental profile (Pitts 1980); o Saffman-Taylor solution (2-7); Δ Pitts solution (2-8); • numerical results.

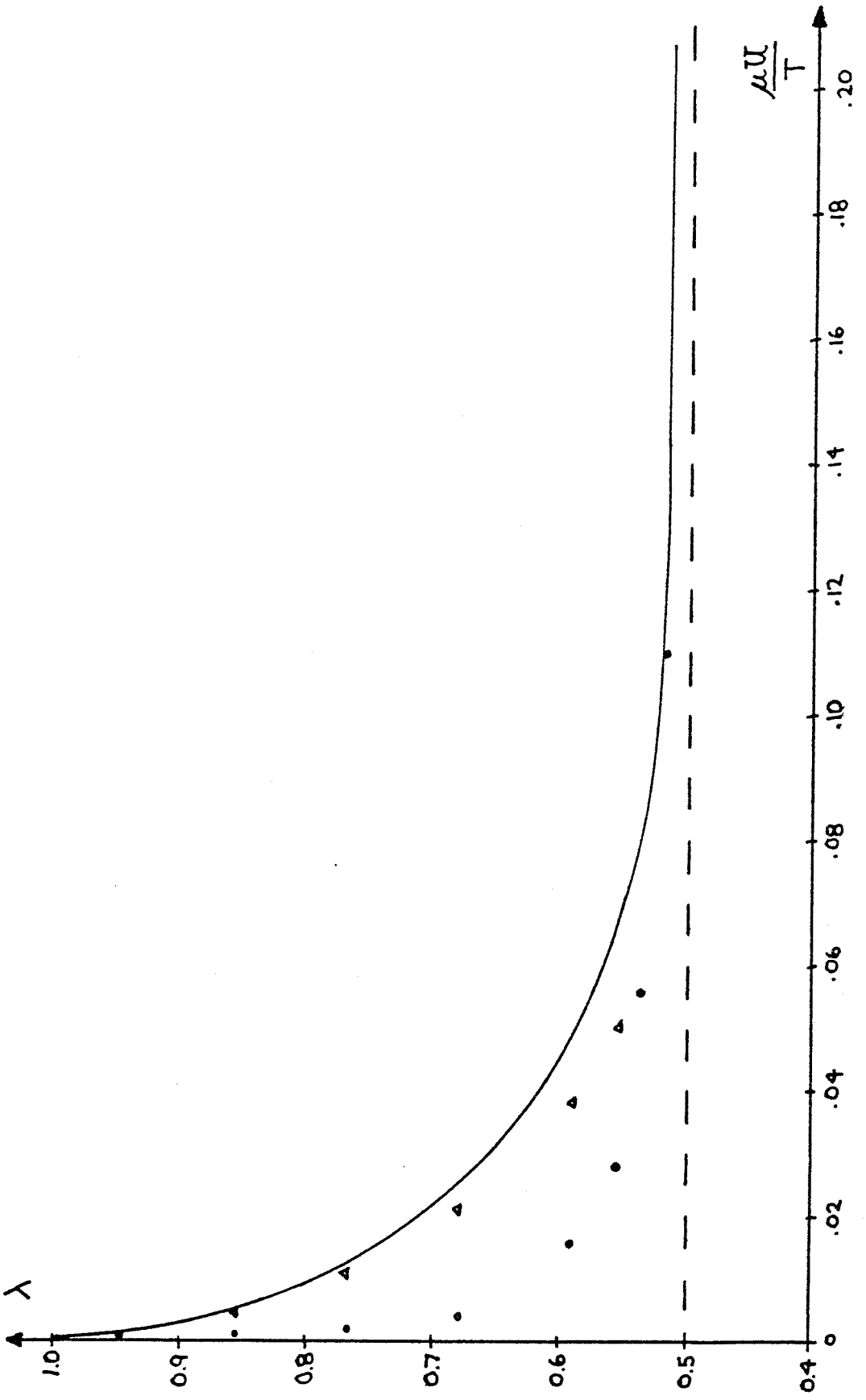

Figure 4-5 Finger width λ versus $\mu U/T$. Solid line: experimental data (Saffman-Taylor 1958); Δ data corrected for finite gap effects; • numerical results.

TABLE 1

		N = 50		N = 100		N = 200		
τ	k	λ_a	λ_b	λ_a	λ_b	λ_a	λ_b	$\mu U/T$ †
.495	.064	.51167	.51179	.51411	.51414	.51496	.51497	.2168
.49	.131	.52309	.52320	.52361	.52364	.52376	.52377	.1098
.48	.273	.53659	.53670	.53677	.53680	.53682	.53683	.0557
.46	.597	.55682	.55691	.55691	.55693	.55693	.55694	.0278
.43	1.21	.58162	.58169	.58166	.58168	.58168	.58169	.0154
.40	2.03	.60405	.60411	.60408	.60409	.60409	.60409	.0103
.35	4.16	.64044	.64048	.64046	.64048	.64047	.64048	.0082
.30	8.07	.67842	.67846	.67845	.67847	.67846	.67847	.0039
.25	16.0	.72001	.72006	.72005	.72006	.72006	.72006	.0026
.20	34.4	.76678	.76682	.76681	.76682	.76682	.76682	.0017
.16	71.1	.80881	.80885	.80883	.80885	.80884	.80885	.0013
.12	175	.85546	.85550	.85548	.85549	.85549	.85549	.0008
.10	308	.88051	.88055	.88053	.88054	.88054	.88054	.0007
.08	609	.90633	.90657	.90655	.90657	.90656	.90656	.0006
.06	1456	.93316	.93320	.93318	.93319	.93318	.93319	.0005
.05	2526	.94647	.94651	.94649	.94650	.94650	.94650	.0005
.04	4947	.95957	.95960	.95959	.95960	.95960	.95960	.0004
.03	11750	.97219	.97222	.97221	.97222	.97222	.97222	.0004
.025	20330	.97820	.97822	.97822	.97822	.97822	.97822	.0003
.02	39740	.98390	.98392	.98392	.98393	.98392	.98393	.0003

λ_a - λ calculated from (4-5)

λ_b - λ calculated from (4-4)

† $\frac{\mu U}{T} = \frac{\pi^2}{12} \left(\frac{b}{a}\right)^2 \left(\frac{1}{1-\lambda}\right)^2 \left(\frac{1}{k}\right)$

for Saffman-Taylor experiment: b = 0.08 cm, a = 1.27 cm

seen in Figure 4-5, this correction cannot fully account for the experimental and numerical discrepancy.

Since the computed profiles agree so well with experiments, there seems to be little doubt of the form of the boundary condition (2-5). Further experimental work is necessary to obtain the appropriate values of t and $T^{\dagger}$, and to understand the discrepancy in Fig. 4-5.

---

† In the Saffman-Taylor experiment, T is measured by measuring the rise of fluid in a capillary tube. There is some question whether this measurement is appropriate in a nonstatic situation.

5. PERTURBATION SOLUTION

Both experimental results for small surface tension and numerical results for small k suggest that the solution to (2-19) varies smoothly with k (Fig. 5-1). The nonuniqueness of (2-19) for $k = 0$ poses some questions, but from experimental and numerical experience we will assume the solution to (2-19) may be expanded in k.

The local analysis of the solution about $s = 0$ shows that the exponent of s depends upon k, so that the solution about $s = 0$ is nonuniform in k. We therefore construct an "inner-outer" matched asymptotic expansion. The inner expansion is given by (3-9). We assume the outer solution may be expanded in powers of k:

$$\begin{aligned} \theta &= \theta_0 + k\theta_1 + k^2\theta_2 + \cdots \\ q &= q_0 + kq_1 + k^2q_2 + \cdots \end{aligned} \tag{5-1}$$

The expansion (5-1) is used in (2-19), and like powers of k are equated:

$$k^0 \begin{cases} q_0 = \cos\theta_0 \\ q_0 = \exp\left\{-\frac{s}{\pi} \mathcal{P}\int_0^1 \frac{\theta_0(s')}{s'(s'-s)}\,ds'\right\} \\ \theta_0(0) = 0 \qquad \theta_0(1) = -\pi/2 \\ q_0(0) = 1 \qquad q_0(1) = 0 \end{cases} \tag{5-2}$$

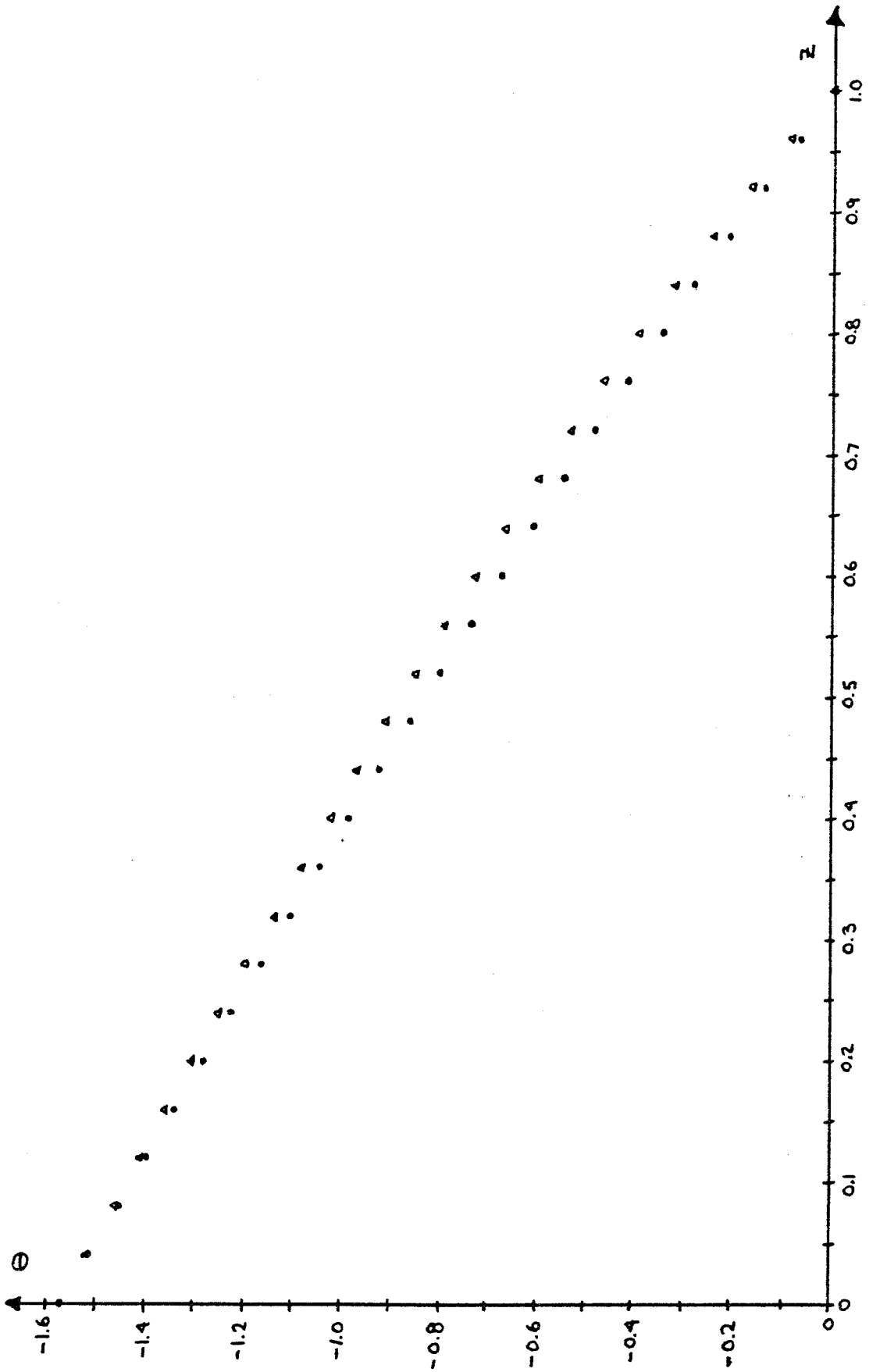

Figure 5-1 Variation of the solution with surface tension. • Saffman-Taylor solution evaluated at $\lambda = \frac{1}{2}$; ▲ numerical results for k=0.273.

$$k^1 \begin{cases} q_1 = q_0 s \frac{d}{ds}\left(q_0 s \frac{d\theta_0}{ds}\right) - \theta_1 \sin\theta_0 \\ q_1 = q_0\left(-\frac{s}{\pi} \fint_0^1 \frac{\theta_1(s')}{s'(s'-s)} ds'\right) \\ \theta_1(0) = \theta_1(1) = 0 \\ q_1(0) = q_1(1) = 0 \end{cases} \tag{5-3}$$

The leading order term in the expansion is the Saffman-Taylor solution (2-22). Eliminating q_1 in (5-3) we obtain a singular linear integral equation for θ_1:

$$\fint_0^1 \frac{\theta_1(s')}{s'-s} ds' = f(s)\theta_1(s) - g(s) \tag{5-4}$$

where:

$$f(s) = \pi \tan\theta_0$$

$$g(s) = \pi s \frac{d}{ds}\left(q_0 s \frac{d\theta_0}{ds}\right) - A$$

$$A = \int_0^1 \frac{\theta_1(s')}{s'} ds'$$

= constant to be determined a posteriori

The solution of this integral equation may be written down explicitly (Carrier, Krook, and Pearson 1966):

$$\theta_1(s) = \frac{f(s)g(s)}{f^2+\pi^2} + \frac{e^{w(s)}}{\sqrt{f^2+\pi^2}} \fint_0^1 \frac{g(s')}{s'-s} \frac{e^{-w(s')}}{\sqrt{f^2+\pi^2}}\, ds'$$

$$+ c \frac{e^{w(s)}}{(1-s)\sqrt{f^2+\pi^2}} \tag{5-5}$$

where:

c = arbitrary constant

$$w(s) = \frac{1}{2\pi i} \fint_0^1 \frac{1}{s'-s} \ln\left(\frac{f(s')+\pi i}{f(s')-\pi i}\right) ds'$$

with the branch of the logarithm chosen so that:

$$0 < \frac{1}{2\pi i} \ln\left(\frac{f+\pi i}{f-\pi i}\right) < 1 \tag{5-6}$$

The integrals in (5-5) may be evaluated explicitly (Appendix C). The constant c is chosen so that θ_1 is finite at $s=0$. The solution to (5-4) is:

$$\theta_1(s) = \frac{\sqrt{1+\phi}}{\pi} \frac{\sqrt{s(1-s)}}{1+s\phi} \left\{ A\left(1 + \frac{1}{\sqrt{1+\phi}}\right) + \frac{\pi\sqrt{1+\phi}}{4} \frac{\sqrt{s}}{(1+s\phi)^{5/2}} (1-2s\phi) \right.$$

$$+ \frac{1}{2(1+s\phi)^2} \left[\frac{1+2\phi-s\phi(\phi+2)}{\phi+1} \right.$$

$$\left.\left. - \frac{\sqrt{1-s}\,(2\phi s-1)}{2\sqrt{1+\phi s}} \log\left(\frac{s(1+\phi)}{2\sqrt{(1-s)(1+\phi s)} + (\phi-1)s+2} \right) \right] \right\} \tag{5-7}$$

Note that $\theta_1(s)$ satisfies the boundary conditions in (5-3).

To determine the constant A, we divide (5-7) by s and integrate from zero to one. All terms of the integration cancel out, leaving A undetermined. This merely points out the fact that the homogeneous problem:

$$\mathcal{F}\int_0^1 \frac{\theta(s')}{s'-s}\,ds' = f(s)\,\theta(s) + \int_0^1 \frac{\theta(s')}{s'}\,ds' \qquad (5\text{-}8)$$

has a nontrivial solution.

It is remarkable that (5-3) has a solution with no restriction on the inhomogeneous term. Since the homogeneous equation (5-8) has a solution, one would expect a solvability condition (Fredholm alternative) to apply to the inhomogeneous term. The only restriction on the inhomogeneous term is that it vanish at $s = 0$. An examination of $g(s)$ (Appendix C) shows that this condition is automatically satisfied for arbitrary ϕ.

At each order of the perturbations, we obtain an equation of the form (5-4), with a different inhomogeneous term. As long as the inhomogeneous term vanishes at $s = 0$, it is possible to obtain a solution which satisfies the boundary conditions (5-3). Each term in the expansion will contain an additional undetermined parameter, corresponding to the homogeneous solution (5-8).

A local expansion about $s = 0$ of $\theta_0(s)$ begins with $\sqrt{s}$, while $\theta_1(s)$ begins with $\sqrt{s}\log s$. In general, the nth order term $\theta_n(s)$ begins with $\sqrt{s}\,\log^n s$. The expansion (5-1) is thus nonuniform at $s = 0$ and must be interpreted as an outer expansion which must be matched to the local behavior about $s = 0$.

We expand the outer solution (2-22) and (5-7) about s = 0:

$$\theta_0(s) = -\sqrt{1+\phi}\ \sqrt{s}\left(1+\frac{s}{6}(1-2\phi)+Os^2\right)$$

$$\theta_1(s) = \frac{\sqrt{1+\phi}}{\pi}\sqrt{s}\left[A\left(1+\frac{1}{\sqrt{1+\phi}}\right)+\frac{1}{2}\frac{1+2\phi}{1+\phi}+\frac{1}{4}\log\left(\frac{1+\phi}{4}\right)\right.$$

$$\left.+\frac{1}{4}\log s\right]+\frac{1+\phi}{4}s+O\left(s^{3/2}\log s\right) \qquad (5\text{-}9)$$

Similarly, we expand the inner solution (3-9) in powers of k. Using (3-8):

$$\tau = \frac{1}{2} - \frac{k}{4\pi} + O(k^2)$$

$$a_2 = \frac{ka_1^2}{4}\left(1+k(\tfrac{1}{4}-\tfrac{1}{\pi})+O(k^2)\right) \qquad (5\text{-}10)$$

The inner solution is:

$$\theta(s) = a_1 s^{\frac{1}{2}-\frac{k}{4\pi}+O(k^2)} + \frac{ka_1^2}{4}\, s^{1-\frac{k}{2\pi}+O(k^2)} + O(s, s^{3\tau})$$

$$= a_1\sqrt{s}\left(1-\frac{k}{4\pi}\log s+\frac{k^2\log^2 s}{32\pi^2}+O\left((k\log s)^n\right)\right.$$

$$\left.+\frac{ka_1^2}{4}s\left(1-\frac{k}{2\pi}\log s+O\left((k\log s)^n\right)\right)\right.$$

$$+\Phi_1 s+O(k^2) \qquad (5\text{-}11)$$

We now match terms. The coefficient a_1 is determined by matching the $\sqrt{s}$ terms of (5-9) and (5-11):

$$a_1 = -\sqrt{1+\phi}+O(k) \qquad (5\text{-}12)$$

We compare the $\sqrt{s}\log s$ term:

$$-\frac{ka_1}{4\pi} = k\,\frac{\sqrt{1+\phi}}{4\pi} + O(k^2) \tag{5-13}$$

Using (5-12), we see that this term is matched. The terms linear in s yield:

$$\frac{ka_1^2}{4} + \Phi_1 = k\,\frac{1+\phi}{4} + O(k^2) \tag{5-14}$$

In the local expansion (3-9), we allowed for the possibility of terms linear in s. From (5-14), we see that the coefficient Φ_1 is at most $O(k^2)$. A closer examination of this term in the local analysis reveals that it will generate additional singularities of the form $s\log^n s$ from (2-19b) (see (B7) in Appendix B). Since these terms cannot be matched, we conclude that $\Phi_1 \equiv 0$. The inner expansion is therefore:

$$\begin{aligned}\theta(s) = {}& {}_1a_1 s^{\tau_1} + {}_1a_2 s^{2\tau_1} + {}_1a_3 s^{3\tau_1} + \cdots \\ & + {}_2a_1 s^{\tau_2} + {}_2a_2 s^{2\tau_2} + \cdots \\ & + \cdots\end{aligned} \tag{5-15}$$

Where τ_2 is the next solution to (3-8):

$$\tau_2 = \frac{3}{2} - \frac{9}{4\pi}k + O(k^2)$$

We expand (5-15) as a power series in k:

$$\theta(s) = {}_1a_1\, s^{1/2}\left(1 - \frac{k}{4\pi}\log s + \cdots\right)$$

$$+ {}_1a_2\, s\left(1 - \frac{k}{2\pi}\log s + \cdots\right)$$

$$+ {}_1a_3\, s^{3/2}\left(1 - \frac{3k}{4\pi}\log s + \cdots\right) \qquad (5\text{-}16)$$

$$+ {}_2a_1\, s^{3/2}\left(1 - \frac{9k}{4\pi}\log s + \cdots\right)$$

$$+ \cdots$$

The local analysis determines ${}_1a_3$ as a function of ${}_1a_1$:

$${}_1a_3 = \frac{{}_1a_1^3}{6}\left(\frac{5}{2} - O(k^2)\right)$$

The constant ${}_2a_1$ is undetermined.

The inner-outer matching may be continued. Comparing the $s^{3/2}$ term, matching can be accomplished with the proper choice of ${}_2a_1$. In a similar manner, the term $s^{2n+1/2}$ can be matched by choosing the coefficient ${}_na_1$ of the s^{τ_n} term. There are enough extra constants to allow matching of these terms to arbitrarily high order.

Once the $s^{2n+1/2}$ terms are matched, all of the constants in the local expansion are determined. We are left to compare the logarithmic singularities. We have shown that the $\sqrt{s}\log s$ term is matched to $O(k^2)$ (5-13). To match the more singular terms (e.g., $\sqrt{s}\log^n s$), it is necessary to compute the $O(k^n)$ term in the outer

expansion. Although possible to do so, the labor would be prohibitive. Instead, we keep track only of the most singular terms in $\theta_2(s)$. We find:

$$\theta_2(s) = -\frac{\sqrt{1+\phi}}{32\pi^2}\sqrt{s}\,\log^2 s + O\left(\sqrt{s}\log s\right) \tag{5-17}$$

By comparison with (5-11), we see that this term is matched with the inner expansion.

With enough fortitude, terms may be compared at any order. To summarize, we have shown that the following terms match:

$s^{2n+1/2}$	-	matched at all orders
$\sqrt{s}\log s$	-	matched at $O(k)$
$\sqrt{s}\log^2 s$	-	matched at $O(k^2)$
s	-	matched at $O(k)$

The width of the finger is given by:

$$\log(1-\lambda) = \frac{1}{\pi}\left\{\int_0^1 \frac{\theta_0(s')}{s'}\,ds' + k\int_0^1 \frac{\theta_1(s')}{s'}\,ds' + \cdots\right\}$$

let:

$$\lambda = \lambda_0 + k\,\lambda_1 + O(k^2)$$

We have:

$$\lambda_0 = \frac{\sqrt{\phi+1}}{\phi}\left(\sqrt{\phi+1} - 1\right)$$

$$\lambda_1 = -\frac{1-\lambda_0}{\pi} A \qquad (5\text{-}18)$$

Note in particular that λ_0 and λ_1 are both undetermined. In fact, we can expect to get an additional arbitrary constant at each order of the perturbation expansion from the homogeneous solution to (5-8).

The width of the finger is also given by (2-21). It can be shown that the perturbations satisfy (2-21) to O(k).

The width of the finger is not determined by the perturbation expansion to the order considered. This presents a conflict with the numerics, which suggest that (2-19) does have a unique solution for $k \neq 0$.

The perturbation expansion is peculiar for two reasons. Since the homogeneous problem (5-8) has a nontrivial solution, we would expect a solvability condition (Fredholm alternative) to fix the parameter ϕ in $\theta_0(s)$. In this problem, the inhomogeneous term vanishes at $s = 0$, and the solvability condition is automatically satisfied. The second unusual feature is in the inner-outer matching. We would expect that constants in the outer solution would be fixed by the local matching (Van Dyke 1975). Although some constants are determined, the crucial parameter ϕ apparently remains arbitrary.

6. THE CONFLICT BETWEEN NUMERICS AND PERTURBATIONS

In an effort to resolve the discrepancy between the numerical computations and the perturbation expansion, various numerical "experiments" have been performed. The results have agreed in all cases with the previous numerical calculations, but have not shed any light on this discrepancy.

The major assumption in the perturbation expansion (5-1) is that the outer solution has a power series expansion in k. This assumption implies that λ also has a power series expansion in k. To investigate this hypothesis, computations were performed for small k. As $k \to 0$, the Jacobian becomes singular, and it is necessary to use a large number of mesh points to obtain a reliable solution (independent of mesh spacing). As a result, computations become very costly for small k, and cost considerations introduce a practical lower bound for the computations.

Computations were performed down to $k = 0.038$. Using 100, 200, and 250 mesh points, the computed value of the width varied by 1%. For larger values of k, the width varied no more than 0.1%. The results are plotted in Figure 6-1. The λ-k plot neither confirms nor denies the form of the expansion (5-1). In particular, it is not clear whether the curve approaches $k = 0$ with finite slope.

As a second test, the parameters ϕ and A are chosen to fit Figure 6-1. With these values used in (2-22) and (5-7), the first two terms of the outer expansion may be compared with the numerics for

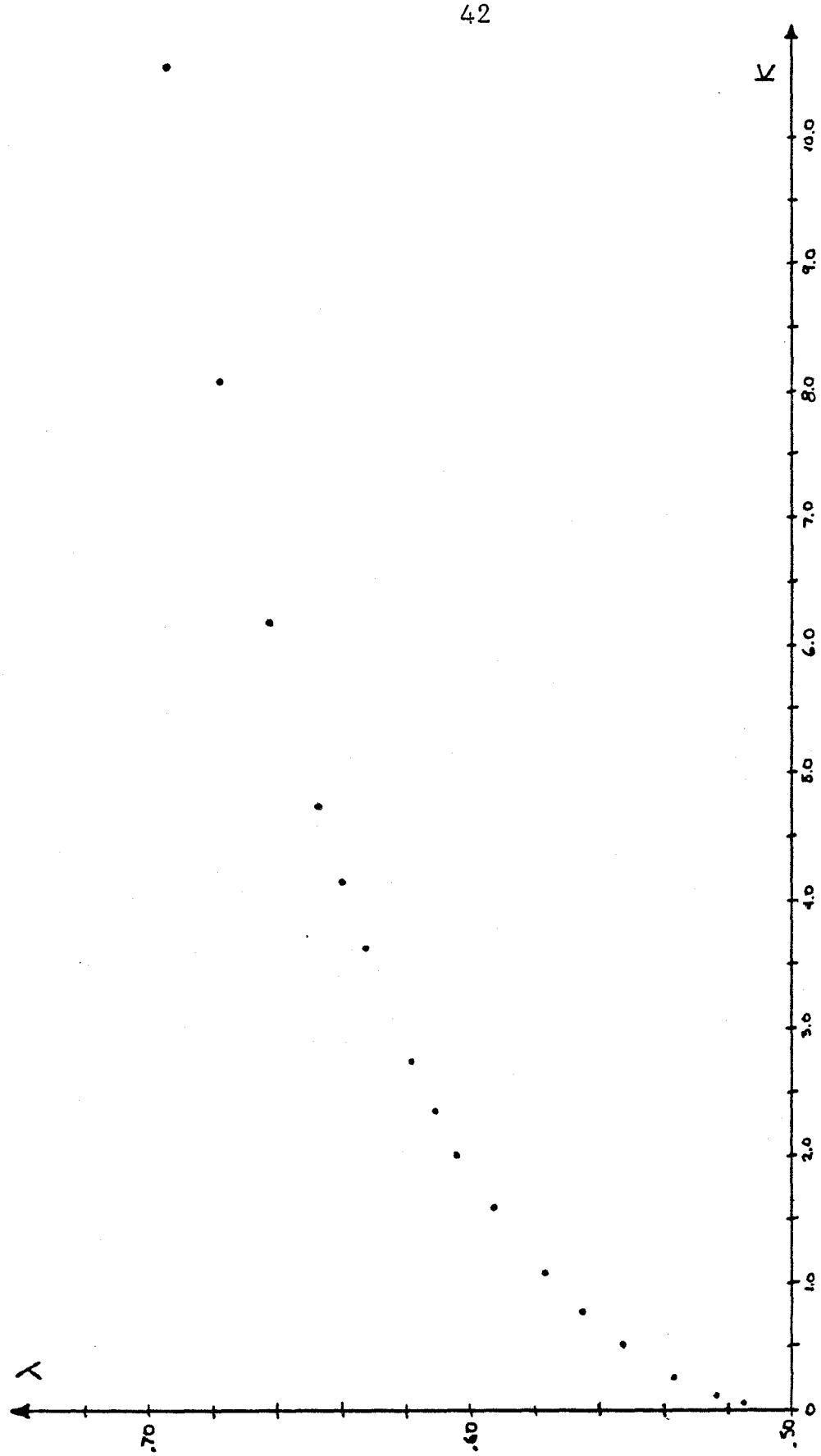

Figure 6-1 Numerical results: variation of λ with k.

small k. With the proper choice of ϕ and A, the numerics and perturbations indicate consistency for small k, but no conclusions may be drawn.

The perturbation analysis and the local expansion about s = 0 both suggest that the coefficient, ${}_1a_1$ of the s^{τ_1} term is arbitrary. To test this feature, we use the first two terms of the local expansion (5-15) to approximate the value of θ at $s = s_1$. Recall that s = 0 corresponds to z = 1 in the "numerical" variables (4-1). The local expansion gives a value for θ at $z = z_1$ depending on ${}_1a_1$, where z_1 is one of the mesh points $\{1\text{-}h,\ 1\text{-}2h,\ 1\text{-}3h\}$. This is used as a boundary value, and the numerical scheme computes a solution on the reduced interval $[0, z_1]$. Experiments have been performed with various values of k, ${}_1a_1$, z_1, and h. A typical result is plotted in Figure 6-2.

As can be seen from the figure, the solution of the "reduced" boundary value problem oscillates, then quickly approaches the solution of the full problem. These oscillations (which are mesh dependent) indicate that a solution to (2-19) does <u>not</u> exist for arbitrary ${}_1a_1$.

Equation (2-20) determines the width λ after θ and q have been determined from (2-19). The perturbations suggest that λ is arbitrary. Using Lagrange multipliers, we include the extra equation (2-20) into the numerical scheme. Consider the system:

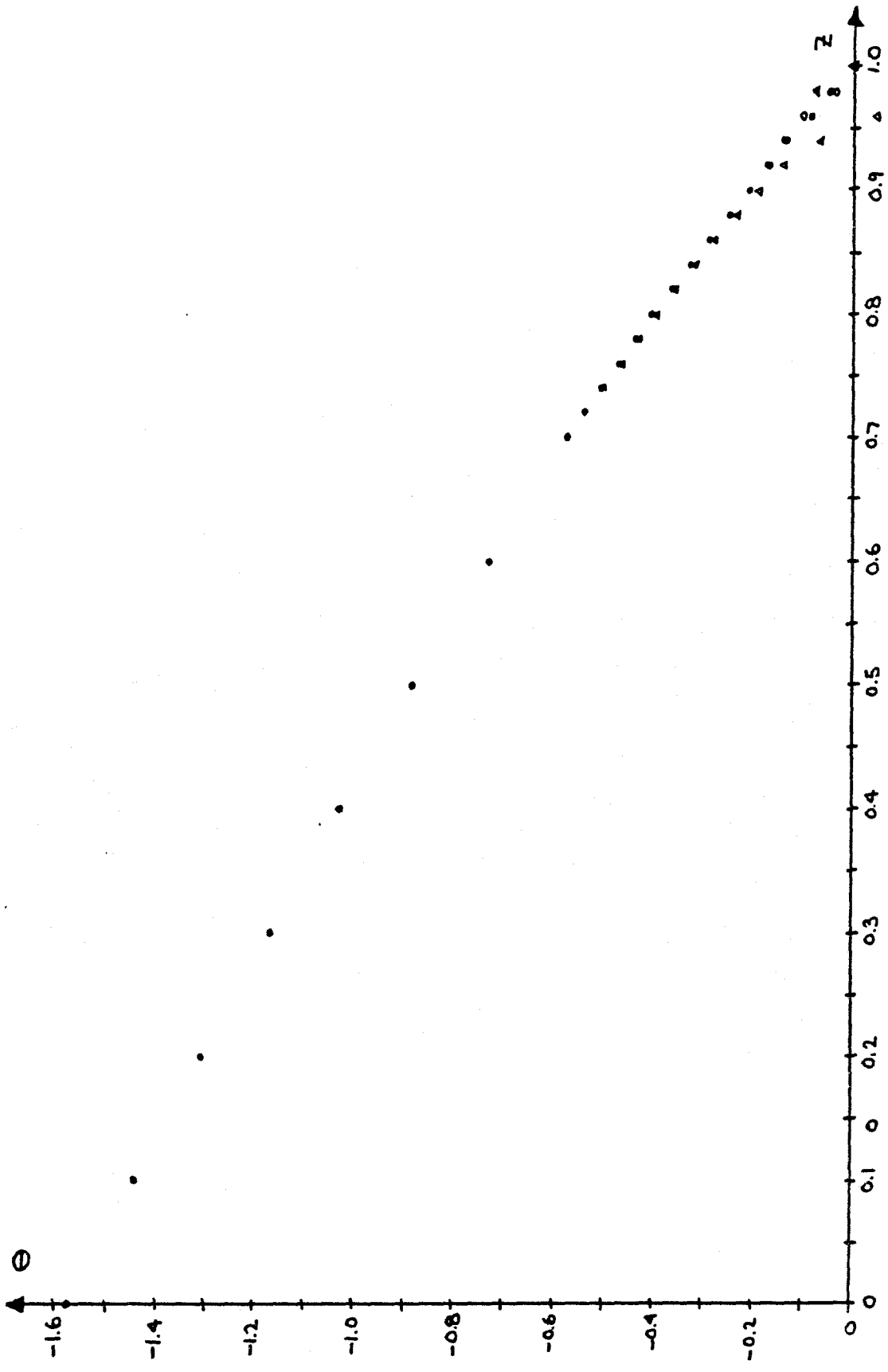

Figure 6-2 Solution of reduced problem for k=0.273, z_1 =0.98, h=.02. • solution to full problem; ▲ reduced problem $_1a_1$ =-2.0; ∘ reduced problem $_1a_1$ =-1.0.

$$q - \cos\theta - kqs\frac{d}{ds}\left(qs\frac{d\theta}{ds}\right) - \alpha f(s) = 0$$

$$\log q = -\frac{s}{\pi}\,\mathcal{P}\int \frac{\theta(s')}{s'(s'-s)}\,ds' \qquad (6\text{-}1)$$

$$\log(1-\lambda) = \frac{1}{\pi}\int_0^1 \frac{\theta(s')}{s'}\,ds'$$

$$\theta(0) = 0 \qquad \theta(1) = -\pi/2$$

where f(s) is an arbitrary function which vanishes at the endpoints. The coefficient α is an extra variable to be determined by the calculations. A solution to the original system (2-19) will correspond to $\alpha = 0$.

The numerical treatment of (6-1) is identical to the treatment of (2-19). The function f is taken to be:

$$f(z) = z(1-z^2) \qquad (6\text{-}2)$$

We choose λ and k and compute the solution $\{\theta;\alpha\}$. The width λ is varied for given k until $\alpha = 0$, which corresponds to a solution of (2-19). A typical λ - α plot is given in Figure 6-3. For $\tau = 0.49$, the curve passes through $\alpha = 0$ when $\lambda = 0.523$. The numerical result for the system (2-19) indicates that $\lambda = 0.524$ for $\tau = 0.49$.

No inconsistencies have been discovered in either the numerics or the perturbations. In the numerics, the replacement of the continuous equations (2-19) by a system of finite difference approximations

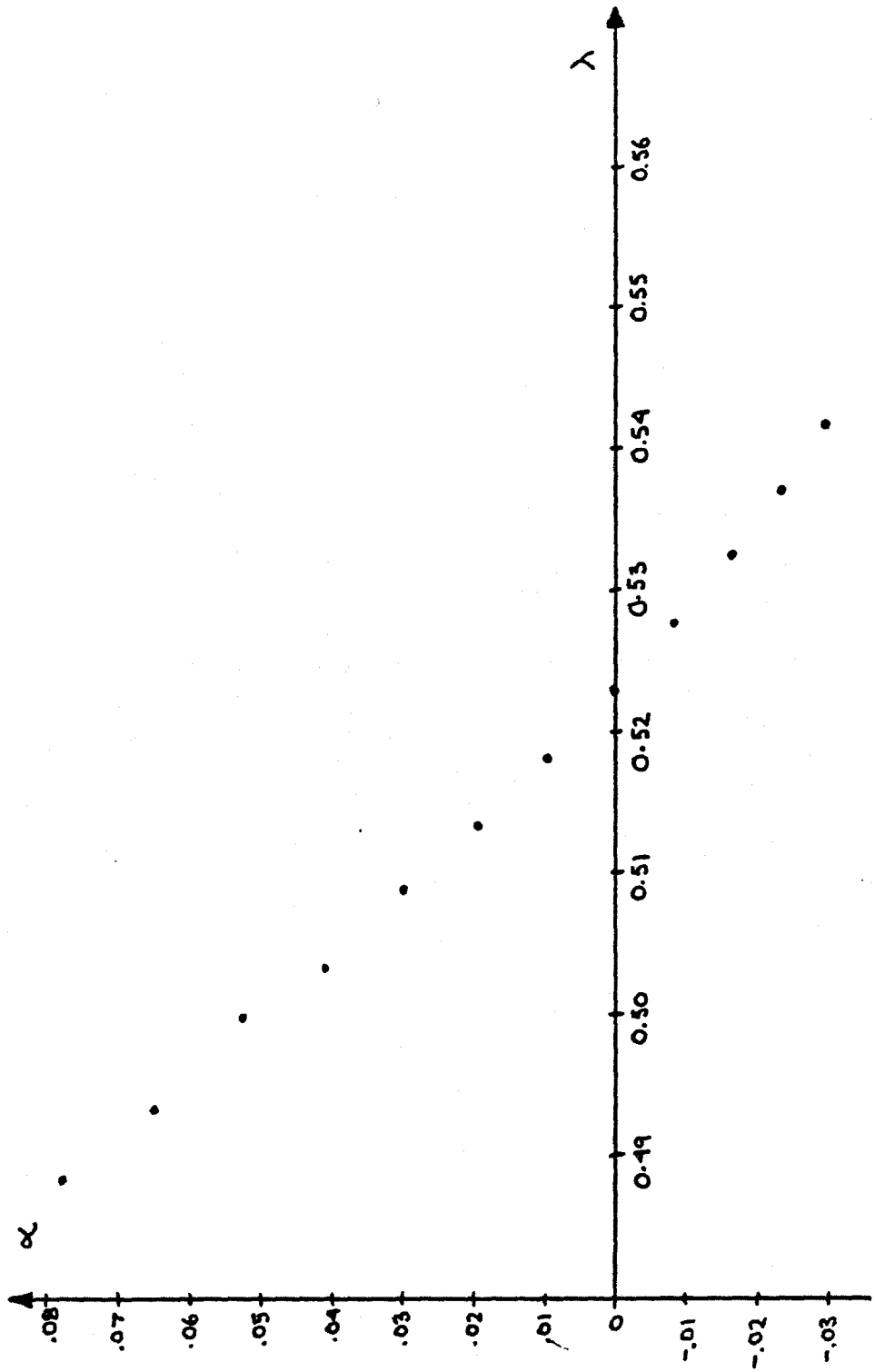

Figure 6-3 Solution of inflated system (6-1) using fifty mesh points.

is open to question. In the perturbations, the form of the expansion (5-1), the convergence of the expansion, the possible appearance of transcendentally small terms, and the possibility that terms cannot be matched at higher orders are all unanswered questions.

This author believes that the numerics are correct, and the perturbations are somehow inadequate. The volume of numerical computations and the excellent agreement of the numerics and experiments lead to this belief. An independent investigation is necessary to confirm or deny this proposition.

7. LINEARIZED STABILITY ANALYSIS

We wish to investigate the stability of the interface between two fluids. We consider small, time dependent perturbations of a steady flow. For small perturbations, we use a linearized analysis. Two cases are considered: the plane interface, and the steady finger.

The stability of a plane interface in a Hele-Shaw cell has been studied by Taylor and Saffman (1958). We reproduce their results here for the purpose of discussion. Consider two fluids propagating in the cell with velocity U:

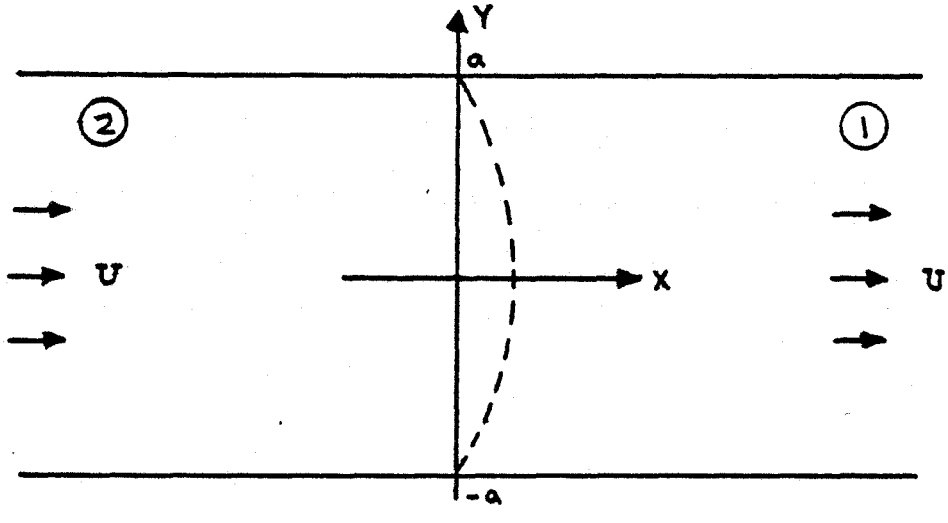

Figure 7-1

The interface is perturbed by a disturbance:

$$x = A_n e^{\sigma t} e^{i \frac{n\pi y}{a}} \tag{7-1}$$

At the interface, the normal component of velocity is continuous, the free surface must satisfy a kinematic condition, and there is a condition on the pressure. The linearized form of these boundary conditions is:

$$\frac{\partial \phi_1}{\partial x} = \frac{\partial \phi_2}{\partial x}$$

$$\frac{\partial \phi}{\partial x} = \frac{\partial x}{\partial t} \tag{7-2}$$

$$\frac{12}{b^2}\left(\mu_2\phi_2 - \mu_1\phi_1\right) = T\frac{d^2x}{dy^2}$$

to be satisfied on $x=0$. A solution to Laplace's equation satisfying (7-2) may be obtained if σ satisfies:

$$\sigma_n = \frac{n\pi b^2}{12}\frac{1}{a(\mu_1+\mu_2)}\left\{\frac{12U}{b^2}(\mu_1-\mu_2) - \left(\frac{n\pi}{a}\right)^2 T\right\} \tag{7-3}$$

A case of interest is where the driving fluid is a gas, i.e., $\mu_2 = 0$:

$$\sigma_n = \frac{n\pi U}{a} - \left(\frac{b^2}{12\mu}\right)\left(\frac{n\pi}{a}\right)^3 T$$

$$\frac{\sigma_n a}{U} = n\pi\left(1 - \left(\frac{T\pi^2}{12\mu U}\right)\left(\frac{b}{a}\right)^2 n^2\right) \tag{7-4}$$

$$= n\pi\left(1 - kn^2\right)$$

where:

$$k \equiv \left(\frac{T\pi^2}{12\mu U}\right)\left(\frac{b}{a}\right)^2$$

For no surface tension, $(k=0)$, perturbations of all wavelengths grow exponentially. For finite surface tension, the short wavelengths (large n) stabilize. At a finite value of the surface tension parameter, $k=1$, disturbances of all wavelengths become stable. This is illustrated in Figure 7-2.

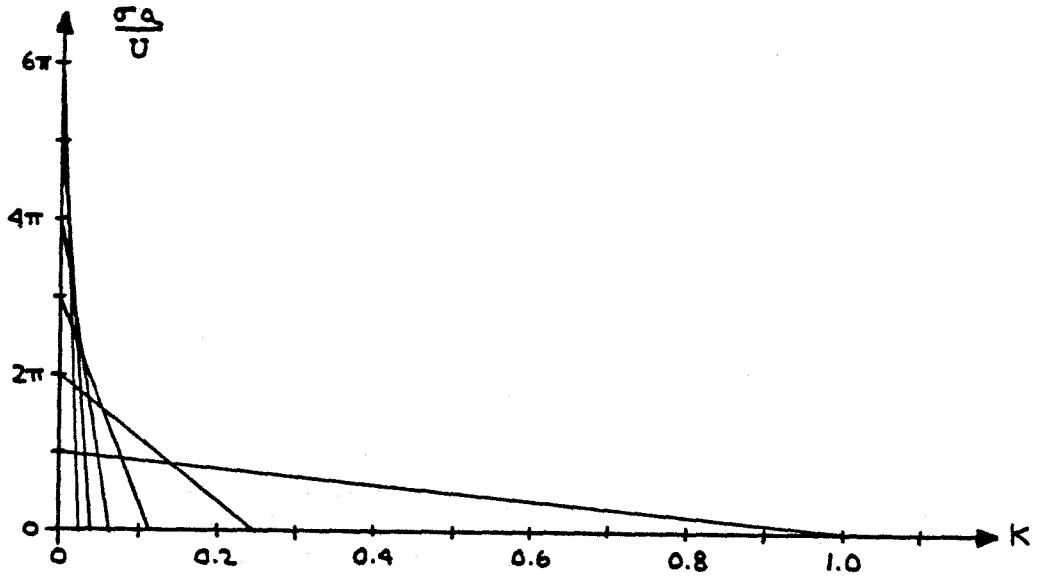

Figure 7-2

We expect that surface tension will have a similar effect when we consider the stability of the fingers. In particular, we expect that the long wavelength perturbations remain unstable longest as the surface tension parameter is increased.

The stability analysis for the finger proceeds in a similar manner. This formulation is identical to the stability investigation of water waves (Longuet-Higgins, 1977).

In the physical plane (Fig. 2-2), the steady finger is bounded by a streamline $\psi = 0$. In the unsteady problem, the interface is described by:

$$x = x_0(\phi, \psi) + \varepsilon\, \xi(\phi, \psi, t)$$

$$y = y_0(\phi, \psi) + \varepsilon\, \eta(\phi, \psi, t) \qquad (7\text{-}5)$$

on $$\psi = \varepsilon F(\phi, t)$$

where: ξ and η are the perturbations of the steady finger x_0, y_0. The free surface is a material surface moving with the fluid, so we have the kinematic condition:

$$\frac{D}{Dt}(\psi - \varepsilon F) = 0 \qquad \text{on} \qquad \psi = \varepsilon F \tag{7-6}$$

where $\frac{D}{Dt}$ is the convective derivative. We write out (7-6):

$$\frac{\partial \psi}{\partial t} + u\frac{\partial \psi}{\partial x} + v\frac{\partial \psi}{\partial y} - \varepsilon\frac{\partial F}{\partial t} - \varepsilon\frac{\partial F}{\partial \phi}\left(\frac{\partial \phi}{\partial t} + u\frac{\partial \phi}{\partial x} + v\frac{\partial \phi}{\partial y}\right) = 0 \tag{7-7}$$

$$\text{on } \psi = \varepsilon F$$

We wish to work in the potential plane, that is, use ϕ and ψ as independent variables. Thus, we must rewrite (7-7) as an equation for x and y (or q and θ) as functions of ϕ and ψ. We have:

$$\begin{aligned} \psi_t &= -\left(\psi_x x_t + \psi_y y_t\right) = v x_t - u y_t \\ \phi_t &= -\left(\phi_x x_t + \phi_y y_t\right) = -u x_t - v y_t \end{aligned} \tag{7-8}$$

Using (7-8) in (7-7), and retaining only terms linear in the perturbations ξ, η, and F, we obtain:

$$F_t + q^2 F_\phi + q\cos\theta\,\eta_t - q\sin\theta\,\xi_t = 0 \tag{7-9}$$

$$\text{on } \psi = 0$$

where q and θ are the velocity and flow angle as defined by (2-11).

The second condition at the interface is the pressure boundary condition (2-10c). We must write an expression for the curvature in the potential plane:

$$\frac{1}{R} = \left| \frac{G_{xx} G_y^2 - 2 G_x G_y G_{xy} + G_{yy} G_x^2}{\left[G_x^2 + G_y^2\right]^{3/2}} \right| \tag{7-10}$$

$$G(x, y) = \psi - \varepsilon F$$

$G = 0$ is the equation of the interface. It is possible to perform the straightforward (but tedious) change of variables to obtain the curvature (7-10) with (ϕ, ψ) as the independent variables:

$$\frac{1}{R} = q\theta_\phi + \varepsilon\left(qF_{\phi\phi} - q_\phi F_\phi\right) + O(\varepsilon^2) \tag{7-11}$$

The pressure boundary condition (2-10c) is

$$\phi = \left(\frac{Tb^2}{12\mu Ua^2(1-\lambda)}\right)\frac{1}{R} - \frac{x}{1-\lambda} \tag{7-12}$$

$$\text{on } \psi = \varepsilon F$$

We use (7-11) in (7-12) and expand $x(\phi, \varepsilon\psi)$ in a Taylor series about $\psi = 0$. Keeping the terms linear in ε, we have:

$$\left(\frac{Tb^2}{12\mu Ua^2}\right)\left\{F\left(q\theta_\phi^2 - q_{\phi\phi} + q_\phi^2/q\right) + qF_{\phi\phi} - q_\phi F_\phi\right\} - \xi + F\frac{\sin\theta}{q} + g(t) = 0 \tag{7-13}$$

$$\text{on } \psi = 0$$

where g(t) is an arbitrary function of time. The independent variable is scaled by (2-15) and the dependent variables are scaled by (2-18). Equations (7-9) and (7-13) become:

$$F_t - \pi s\left(\frac{\tilde{q}}{1-\lambda}\right)^2 F_s = \left(\frac{\tilde{q}}{1-\lambda}\right)\left(\cos\tilde{\theta}\,\eta_t - \sin\tilde{\theta}\,\xi_t\right)$$

$$(1-\lambda)k\left\{F\left(\tilde{q}(s\tilde{\theta}_s)^2 - s\frac{d}{ds}(s\tilde{q}_s) + \frac{(s\tilde{q}_s)^2}{\tilde{q}}\right) + \tilde{q}s\frac{d}{ds}(sF_s)\right. \qquad (7\text{-}14)$$

$$\left. - s^2\tilde{q}_s F_s\right\} - \xi - \frac{F\sin\tilde{\theta}}{\tilde{q}}(1-\lambda) + g(t) = 0$$

We must find a complex function $\xi + i\eta$ which is an analytic function of $s + it$ and satisfies (7-14) on $t = 0$. Let us reconsider the flow in Figure 2-3, this time including the entire finger:

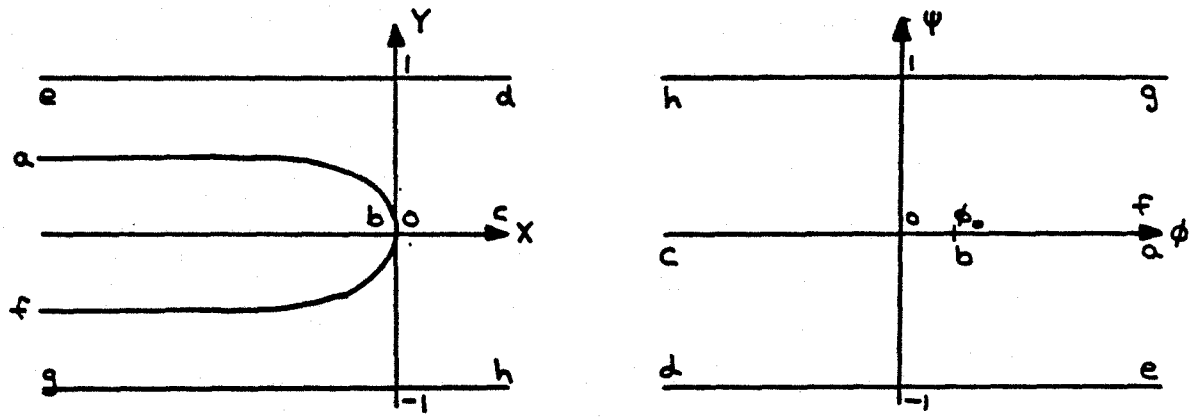

Figure 7-3

We perform a Schwartz-Christoffel transformation to map the potential plane into the upper half plane:

$$w(Z) = \phi + i\psi = -\frac{1}{\pi}\log(1-Z^2) + \phi_0 \qquad (7\text{-}15)$$

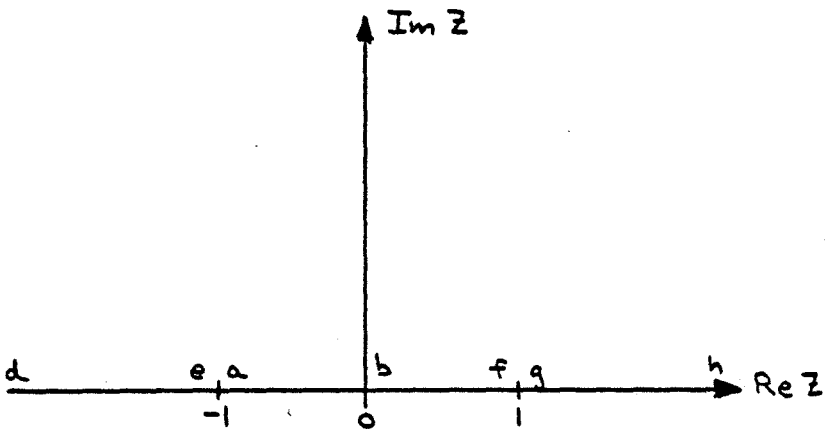

Figure 7-4

where the branches are chosen appropriately.

A second conformal transformation will map the upper half plane onto a strip:

$$Z = \sin\Omega\,, \qquad \Omega = u + iv \qquad (7\text{-}16)$$

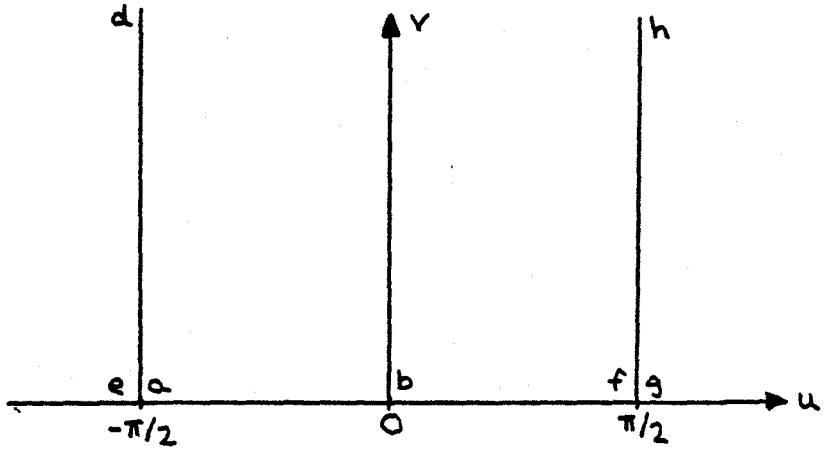

Figure 7-5

To complete the problem, we must describe the boundary conditions to be satisfied by ξ and η along the walls de and hg, and the conditions far upstream dch.

In the unsteady problem, the changing area A of the finger must be balanced by an additional flux of fluid upstream. The boundary condition in the physical plane (Fig. 7-3) becomes:

$$\psi = -1 + \frac{1}{2}\frac{\partial A}{\partial t} + c(t) \qquad \text{on } y = 1$$

$$\psi = 1 - \frac{1}{2}\frac{\partial A}{\partial t} + c(t) \qquad \text{on } y = -1 \tag{7-17}$$

In the potential plane the boundary condition on $\psi = 1$ becomes:

$$1 = y_0\left(\phi, -1 + \frac{1}{2}\frac{\partial A}{\partial t} + c(t)\right) + \varepsilon\eta\left(\phi, -1 + \frac{1}{2}\frac{\partial A}{\partial t} + c(t)\right)$$

$$= y_0(\phi, -1) + \left(\frac{1}{2}\frac{\partial A}{\partial t} + c(t)\right)\frac{\partial y_0}{\partial \psi}(\phi, -1) + \varepsilon\eta(\phi, -1) + O(\varepsilon^2)$$

$$\therefore \qquad \eta(\phi, -1) = -\left(\frac{1}{2}\frac{\partial A}{\partial t} + c(t)\right)\frac{\partial y_0}{\partial \psi}(\phi, -1) \tag{7-18}$$

with a similar boundary condition to hold at $\psi = +1$. $\frac{\partial A}{\partial t}$ can be related to F at the endpoints, and can be shown to be zero (Appendix D). We choose c(t) to be zero. Thus we have:

$$\eta(\phi, -1) = \eta(\phi, 1) = 0 \tag{7-19}$$

We consider symmetric and antisymmetric disturbances separately.

The most general analytic function of Ω which satisfies (7-19) and vanishes upstream is:

<u>symmetric</u>:

$$\xi + i\eta = e^{\sigma t} \sum_{0}^{\infty} a_n e^{2ni\Omega}$$

$$a_n \text{ real} \qquad (7\text{-}20)$$

<u>antisymmetric</u>:

$$\xi + i\eta = e^{\sigma t} \sum_{0}^{\infty} b_n e^{(2n+1)i\Omega}$$

$$b_n \text{ pure imaginary}$$

The coefficients a_n and b_n are chosen to satisfy (7-14) on $v = 0$.

Taylor and Saffman (1958) solved the stability equations for no surface tension. They worked in a frame of reference where the finger is moving. In our frame of reference, we can reproduce their results. We set $k=0$ in (7-14):

$$F = \frac{q}{(1-\lambda)\sin\theta}\{g(t) - \xi\}$$

$$F_t - \pi s\left(\frac{q}{1-\lambda}\right)^2 F_s = \frac{q}{1-\lambda}\left(\cos\theta\eta_t - \sin\theta\xi_t\right) \qquad (7\text{-}21)$$

We eliminate F from (7-21) and use the Saffman-Taylor solution (2-22) for q and θ. For simplicity, we take $\lambda = 1/2$ ($\phi = 0$). The system (7-21) becomes:

$$(1-s)\,\xi_t - \sqrt{s(1-s)}\,\eta_t - g_t + 2\pi\,[\xi - g - 2s(1-s)\,\xi_s] = 0 \qquad (7\text{-}22)$$

For no surface tension, $\phi_0 = 0$, so s can be written in terms of u:

$$s = \cos^2 u \qquad (7\text{-}23)$$

Equation (7-22) becomes:

$$(\sin^2 u)\,\xi_t + (\sin u \cos u)\eta_t - g_t + 2\pi[\xi - g + \cos u \sin u\,\xi_u] = 0 \qquad (7\text{-}24)$$

We consider the symmetric perturbations (7-20):

$$\begin{aligned} \xi &= e^{\sigma t} \sum_0^\infty a_n \cos 2nu \\ \eta &= e^{\sigma t} \sum_0^\infty a_n \sin 2nu \\ g(t) &= e^{\sigma t} g \end{aligned} \qquad (7\text{-}25)$$

Using (7-25) in (7-24) and equating Fourier coefficients, we obtain a recursion relation for the a_n:

$$\begin{aligned} &\underline{n = 0} \qquad 2\pi\left[a_0 - g - \frac{a_1}{2}\right] + \sigma\left[\frac{a_0}{2} - g\right] = 0 \\ &\underline{n > 0} \qquad -\pi(n+1)a_{n+1} + \left(2\pi + \frac{\sigma}{2}\right) a_n + \left(\pi(n-1) - \frac{\sigma}{2}\right) a_{n-1} = 0 \end{aligned} \qquad (7\text{-}26)$$

The series (7-25) will be finite if

$$\sigma = 2\pi m$$
$$m = 0, 1, 2 \cdots \tag{7-27}$$

In particular, $m = 0$ represents uniform translation of the finger, while $m = 1$ is the perturbation:

$$\xi = a_0\left(1 + \frac{1}{3}\cos 2u\right) e^{2\pi t}$$
$$\eta = \frac{a_0}{3} \sin 2u \, e^{2\pi t} \tag{7-28}$$

The eigenfunction associated with the eigenvalue $\sigma = 2\pi m$ will contain the first $(m + 1)$ Fourier components.

This result was first obtained by Taylor and Saffman (1958). Since the eigenvalues σ are all positive, the linearized stability analysis suggests that the fingers are all unstable, a conclusion which does not agree with experimental observations.

To examine the stability of the fingers for nonzero surface tension, we look for numerical solutions of (7-14). We rewrite (7-14) using z as an independent variable, as defined by (4-1). Rather than using F as the dependent variable, it is convenient to use:

$$W \equiv F/q \tag{7-29}$$

which can be shown to be bounded (Appendix D). The equations are:

$$(1-\lambda)k\tau^2\left\{W\left[q\left(\frac{1-z^2}{2z}\right)\theta_z\right]^2 + W_z\left[\frac{1}{2}\frac{d}{dz}\left(q\,\frac{1-z^2}{2z}\right)^2\right]\right.$$

$$\left. + W_{zz}\left[q\left(\frac{1-z^2}{2z}\right)\right]^2\right\} - \xi - W\sin\theta(1-\lambda) + g(t) = 0$$

$$W_t + \frac{\pi\tau}{1-\lambda}\left(\frac{1-z^2}{2z}\right)\frac{q}{1-\lambda}(qW)_z = \frac{1}{1-\lambda}\left(\cos\theta\eta_t - \sin\theta\,\xi_t\right) \qquad (7\text{-}30)$$

The solution q and θ are computed from (4-2) on the upper half of the finger ($0 < z < 1$). Using symmetry, q and θ may be continued for $-1 < z < 0$. The definition of q and θ (2-11) allows for some freedom in choosing their parity. In particular, the only requirement for a symmetric finger is that:

$$u = q\cos\theta = \text{even}$$
$$v = q\sin\theta = \text{odd} \qquad (7\text{-}31)$$

We choose a smooth continuation of q and θ for $-1 < z < 0$ such that:

$$q(-z) = -q(z)$$
$$\sin\theta(-z) = \sin\theta(z) \qquad (7\text{-}32)$$
$$\cos\theta(-z) = -\cos\theta(z)$$

This corresponds to the following picture:

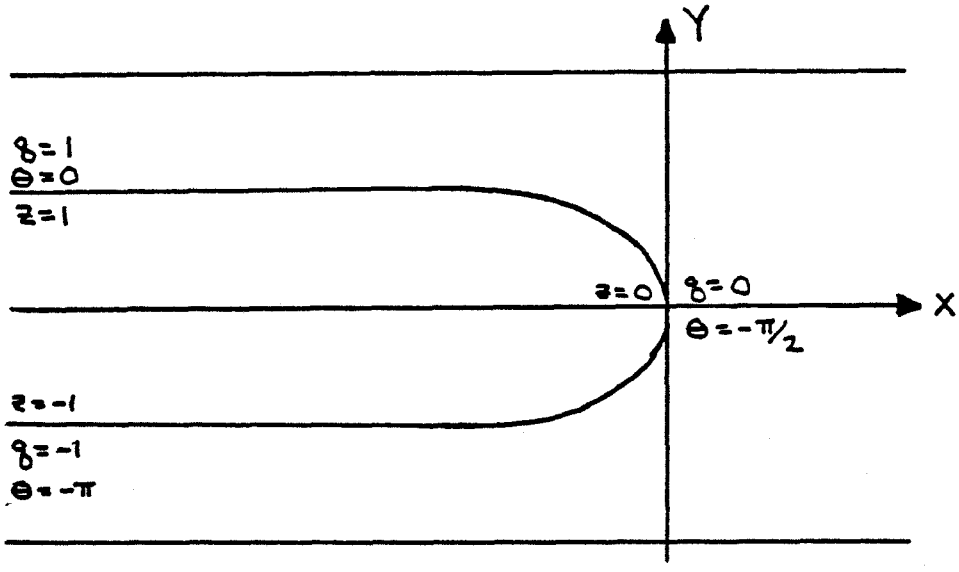

Figure 7-6

Using this continuation for q and θ, it can be seen that the solutions to (7-30) can be divided into symmetric and antisymmetric perturbations. We consider the symmetric perturbations:

$$\xi = e^{\sigma t} \sum_{0}^{\infty} a_n \cos 2nu$$

$$\eta = e^{\sigma t} \sum_{0}^{\infty} a_n \sin 2nu \qquad (7\text{-}33)$$

$$W = e^{\sigma t} \sum_{0}^{\infty} b_n \cos(2n-1)u$$

The form of W is dictated by the requirement that W vanishes at the endpoints.

The relationship between u and z is:

$$\cos u = (1-z^2)^{1/2\tau} \qquad (7\text{-}34)$$

We solve for the coefficients $\{a_n, b_n\}$ by collocation. The series (7-33) is truncated at a finite number of Fourier modes, say N, and the coefficients $\{a_n, b_n\}$ are chosen to satisfy (7-33) at N equally-spaced mesh points in (0, 1). This leads to an eigenvalue problem for σ of the form:

$$\left(A_N - \sigma B_N\right) \cdot \begin{pmatrix} a_n \\ b_n \end{pmatrix} = 0 \qquad (7\text{-}35)$$

where A_N and B_N are square matrices of order $(2N \times 2N)$. Since we know the solution to (7-35) when $k = 0$ (e.g., (7-28)), Newton's method is a good choice to follow the eigenvalues for $k > 0$.

The truncation N of the Fourier series is varied to obtain the eigenvalues. Since we know that the smallest eigenvalues include only a few modes for $k = 0$, it should be possible to obtain a good estimate of the eigenvalue using only a few modes for $k > 0$. We have computed the lowest eigenvalue using $N = \{5, 6, 8, 10, 12, 15\}$.

Since the stability equations (7-30) involve second derivatives of W, the truncated system (7-35) is very sensitive to the truncation N, and truncation errors in the coefficients in (7-30). To obtain accuracy in the eigenvalues σ, it is necessary to know the coefficients accurately. For this purpose, we have used a large number of mesh points (240) to compute q and θ. The centered difference quotients in (4-3), although $O(h^2)$ accurate, produce errors in the high harmonics. Richardsen extrapolation helps to suppress these harmonics.

The lowest eigenvalue, following the $\sigma_0 = 2\pi$ branch, has been computed for $0 < k < 1$. With Richardsen extrapolation performed on the coefficients, the computed eigenvalue did not vary more than 1% as the truncation value N was varied. The results are plotted in Figure 7-7. This eigenvalue remains real and positive throughout this range of k, indicating the finger is unstable. Experimental results indicate that the finger is very stable in this range of k.

The two-dimensional, linearized stability analysis predicts that the finger is unstable to small disturbances. This is in variance with experimental observations. A proper treatment of stability should include three-dimensional effects to recover the experimental results.

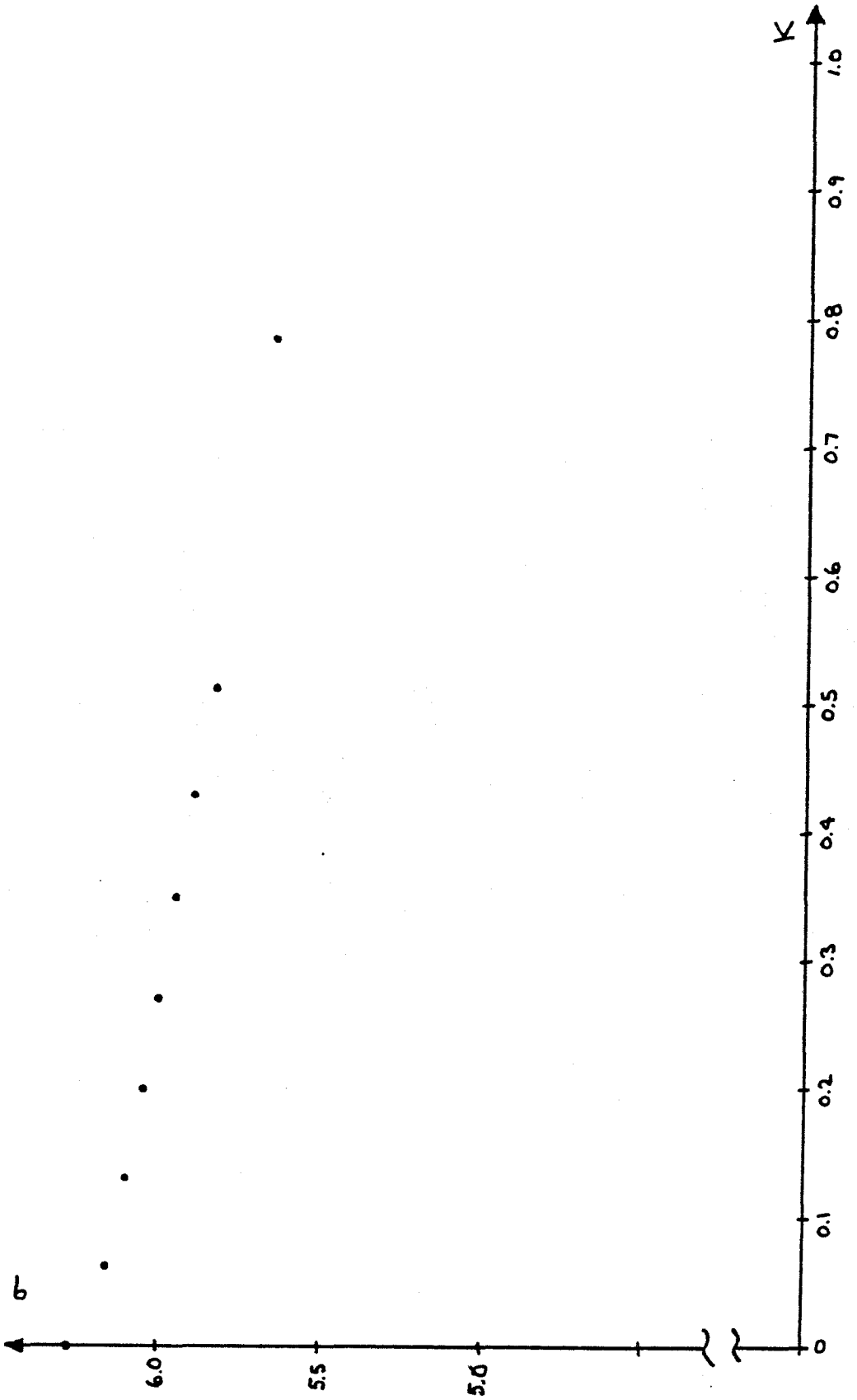

Figure 7-7 Stability results for finite surface tension: the smallest eigenvalue branch.

8. OTHER STEADY SOLUTIONS

We have examined two possible steady shapes for the interface between two fluids in a porous media: the plane interface and the finger. We are interested in other possible steady configurations.

The stability plot, Figure 7-2, shows the eigenvalues σ passing through zero for various values of k. Each of these zero-crossings indicate a new steady state solution. The analysis in the previous chapter was a linearized analysis. We will be interested in continuing these steady-state solutions to finite amplitude.

Consider the following steady flow:

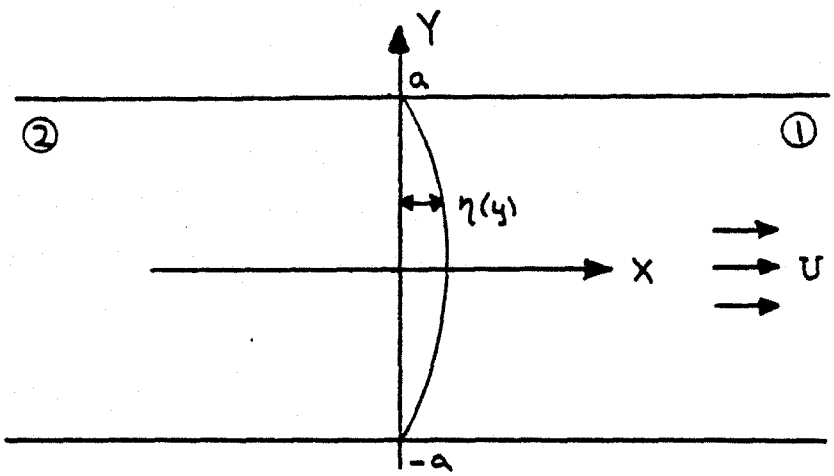

Figure 8-1

The interface is:

$$f(x, y, t) = Ut + \eta(y) - x = 0 \qquad (8\text{-}1)$$

The boundary conditions at the interface are: continuity of normal velocity, the kinematic boundary condition, and the dynamic boundary condition:

$$\frac{\partial \phi_1}{\partial n} = \frac{\partial \phi_2}{\partial n} \tag{8-2a}$$

$$\frac{D}{Dt} f = U - \phi_x + \phi_y \eta_y = 0 \tag{8-2b}$$

$$\mu_2 \phi_2 - \mu_1 \phi_1 = \frac{Tb^2}{12} \frac{\eta_{yy}}{[1+(\eta_y)^2]^{3/2}} + \text{constant} \tag{8-2c}$$

For upstream and along the walls we require:

$$\begin{aligned} &\phi_1 \sim Ux \text{ as } x \to +\infty \\ &\phi_2 \sim Ux \text{ as } x \to -\infty \\ &\phi_y = 0 \quad \text{at } y = \pm a \end{aligned} \tag{8-3}$$

A steady solution which satisfies (8-2) and (8-3) is:

$$\begin{aligned} &\phi_1 = Ux + (\text{constant}) \\ &\phi_2 = Ux + (\text{constant}) \end{aligned} \tag{8-4}$$

Equations (8-2a), (8-2b) and (8-3) are automatically satisfied. (8-2c) becomes:

$$\eta_{yy} + c^2 \left[1 + (\eta_y)^2\right]^{3/2} \eta = 0 \tag{8-5}$$

where $$c^2 = \frac{12U(\mu_1 - \mu_2)}{Tb^2}$$

The solution η is required to be periodic of period 2a. We fix the origin by taking:

$$\eta(a) = \eta(-a) = 0 \tag{8-6}$$

The dependent and independent variables are scaled to make the problem dimensionless:

$$\tilde{\eta} = \eta/a \qquad \tilde{y} = y/a \tag{8-7}$$

Dropping the (~), the scaled equations become:

$$k\eta_{yy} + \left[1 + (\eta_y)^2\right]^{3/2} \eta = 0$$

$$\eta(1) = \eta(-1) = 0 \tag{8-8}$$

$$k = \frac{T}{12U(\mu_1 - \mu_2)} \left(\frac{b}{a}\right)^2 .$$

Equations (8-8) are analyzed by perturbation methods. We take:

$$\begin{aligned} \eta &= \varepsilon\eta_1 + \varepsilon^2\eta_2 + \cdots \\ k &= k_0 + \varepsilon k_1 + \cdots \\ 0 &< \varepsilon << 1 \end{aligned} \tag{8-9}$$

The expansion (8-9) is used in (8-8). We equate like powers of ε:

$$\varepsilon^1: \qquad k_0\eta_{1yy} + \eta_1 = 0$$

$$\eta_1(1) = \eta_1(-1) = 0 \tag{8-10}$$

$$\varepsilon^2: \qquad k_0\eta_{2yy} + \eta_2 = -k_1\eta_{1yy}$$

$$\eta_2(1) = \eta_2(-1) = 0 \tag{8-11}$$

$$\varepsilon^3: \qquad k_0\eta_{3yy} + \eta_3 = -k_2\eta_{1yy} - \frac{3}{2}\eta_{1y}^2\eta_1$$

$$\eta_3(1) = \eta_3(-1) = 0 \tag{8-12}$$

Equation (8-10) has sine and cosine solutions. For simplicity, we consider only the sine solution. The analysis is identical for the cosine solutions. Take:

$$\eta_1(y) = a \sin n\pi y$$

$$k_0 = (1/n\pi)^2 \tag{8-13}$$

This solution is substituted into (8-11) and (8-12). Since we require η to be periodic, we must choose k_1 and k_2 to suppress secular terms, that is, k_1 and k_2 are chosen so that the inhomogeneous terms do not contain multiples of the homogeneous solution. We obtain:

$$k_1 = 0$$

$$k_2 = 3/8\ a^2 \tag{8-14}$$

For the equation (8-8) to have a nontrivial solution, the parameter k must satisfy:

$$k = \left(\frac{1}{n\pi}\right)^2 + \frac{3}{8}(\varepsilon a)^2 + O(\varepsilon^4) \tag{8-15}$$

The linear part of the solution ($\varepsilon = 0$) agrees with the results previously obtained (Fig. 7-2).

For finite amplitude, equations (8-8) are solved numerically. The amplitude of the solution is defined as:

$$||\eta||^2 \equiv \int_{-1}^{1} \eta^2(y)\, dy \tag{8-16}$$

For the perturbation solution:

$$||\eta||^2 = \varepsilon^2 ||\eta_1|| + O(\varepsilon^4)$$

$$= (\varepsilon a)^2 + O\left((\varepsilon a)^4\right) \tag{8-17}$$

We fix the amplitude $||\eta||$, and compute the unknowns $\{\eta_2, \cdots, \eta_N; k\}$ by satisfying (8-16) and (8-8) at the (N-1) interior points. We follow the symmetric and antisymmetric solutions independently. Newton's method is used to compute the solution.

Euler continuation is used to follow the finite amplitude branches. At a finite value of the amplitude, the determinant of the Jacobian changes sign, and the Euler method comes to a halt. It would be possible to follow these branches farther using a more sophisticated continuation scheme, but we have made no effort to do so.

Results have been obtained for a number of the antisymmetric perturbations. The numerical results are plotted along with the perturbation analysis. The lowest order symmetric branch has been followed up to the secondary bifurcation point. The results are plotted in Figures 8-2 and 8-3.

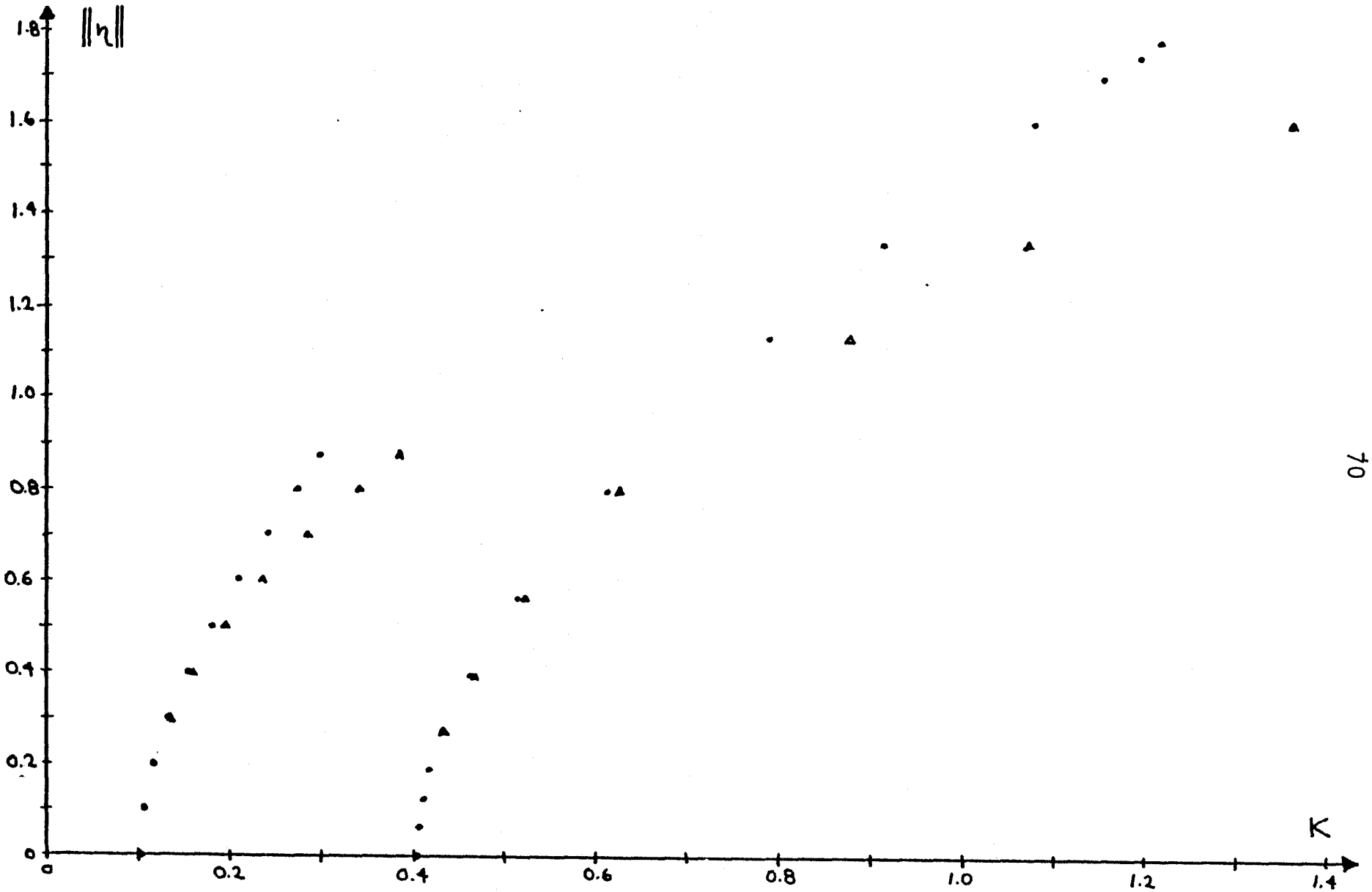

Figure 8-2 Bifurcation from plane interface into other steady shapes. • numerical results (100 mesh points); ▲ perturbation results (8-15). The larger branch is a symmetric perturbation, the smaller is antisymmetric.

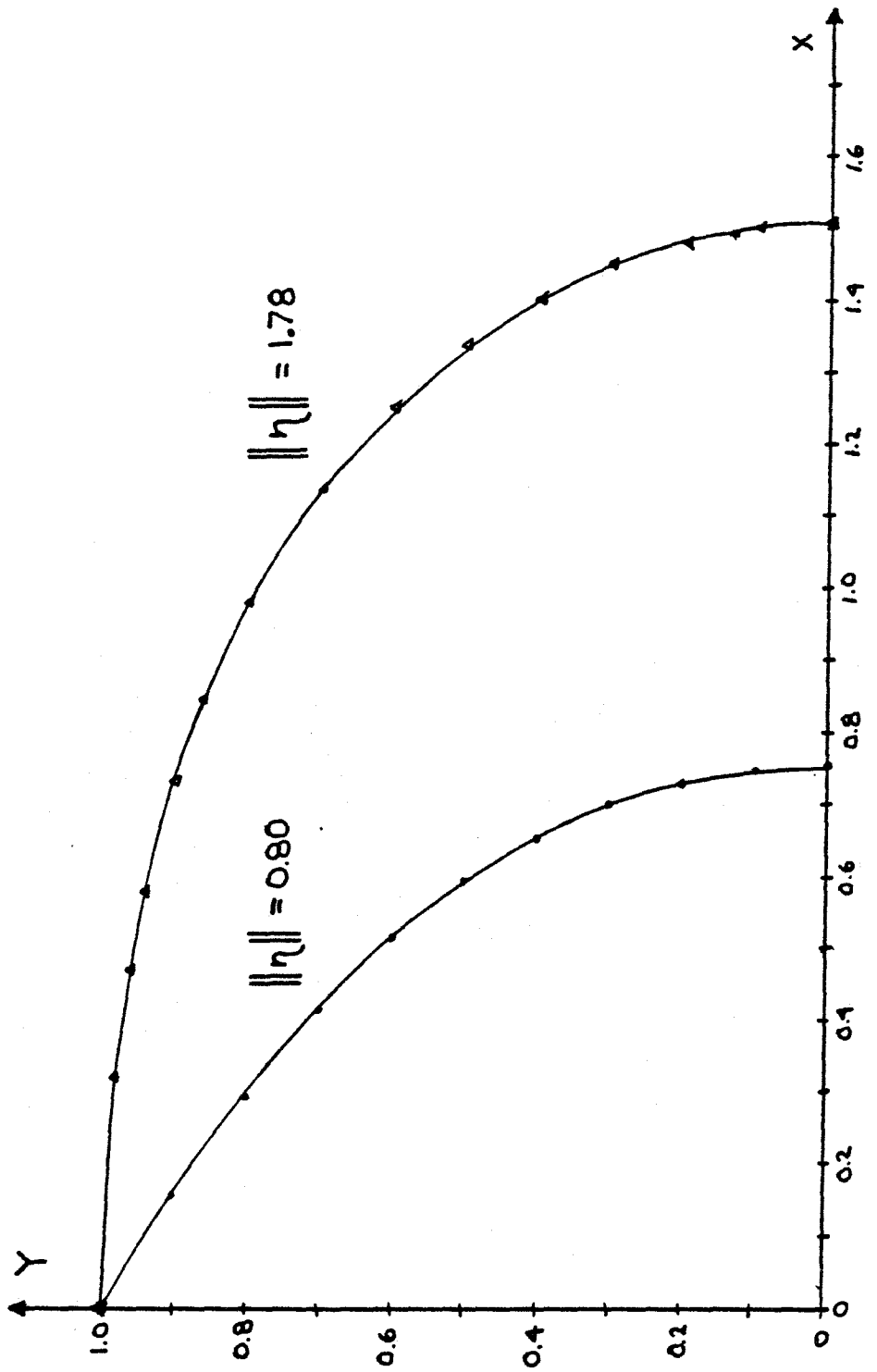

Figure 8-3 Profiles of the symmetric branch.

9. DISCUSSION

We have derived the equations for the shape of the interface between two liquids in a porous medium or a Hele-Shaw cell. A numerical study of these equations suggests that including surface tension in the description of the problem removes the nonuniqueness of the Saffman-Taylor solution. The numerical profiles have been shown to agree with experimental observations.

A perturbation expansion of the solution has been obtained as an expansion in the surface tension parameter. At each order, the terms in the expansion satisfy a singular integral equation, which can be solved in closed form. The expansion is nonuniform and must be matched to an "inner" solution at $s = 0$. To the order considered, the expansion has been shown to be formally self-consistent, but the width of the finger remains undetermined.

The numerical solution and the perturbation expansion yield conflicting results. The discrepancy between the two has not been resolved. Since the numerics and the perturbations are both found to be self-consistent, the resolution of this conflict will require a very subtle analysis. The author favors the numerical results due to the excellent agreement with experiments.

Taylor and Saffman (1958) showed that the fingers are unstable to small disturbances. This instability has not been removed by including surface tension in the analysis. Since this result is at variance with experiments, it is believed that three-dimensional effects must strongly influence the stability of the fingers.

The plane interface and the extended finger are only two possible steady flows. We have briefly considered additional steady profiles. By perturbation methods, we have shown that steady profiles bifurcate from the plane interface at particular values of the surface tension parameter. These bifurcated branches are followed numerically to finite amplitude. The numerical continuation comes to a halt when a sign change is detected in the determinant of the Jacobian, suggesting some sort of secondary bifurcation. The nature of this secondary bifurcation, and the stability of the bifurcated branch have not been investigated.

APPENDIX A

For no surface tension, the solution given by Saffman and Taylor is:

$$z_f = x_f + iy_f = \frac{w_f}{\lambda U} + \frac{2(1-\lambda)}{\pi} a \log \frac{1}{2}\left(1 + e^{-\frac{\pi w_f}{\lambda U a}}\right) + Ut \tag{A1}$$

where $w_f = \phi_f + i\psi_f$ is the potential in the fixed coordinate system. In a frame of reference moving with the finger, we have:

$$w_{moving} = w_f - Uz_{moving}$$
$$z_{moving} = z_f - Ut \tag{A2}$$

$$z_m = \frac{w_m + Uz}{\lambda U} + \frac{2(1-\lambda)}{\pi} a \log \frac{1}{2}\left(1 + e^{-\frac{\pi w_m}{\lambda U a}} e^{-\frac{\pi z}{\lambda a}}\right) \tag{A3}$$

The interface is given by $\psi_m = 0$. An examination of (2-17) for $T = 0$ shows $\phi_0 = 0$, thus:

$$s = e^{-\pi\phi} \tag{A4}$$

Performing the scaling (2-9) and (2-15), we have:

$$2 s^{\frac{1}{2\lambda}} e^{-\frac{\pi\hat{z}}{2\lambda}} = 1 + s^{\left(\frac{1-\lambda}{\lambda}\right)} e^{-\frac{\pi\hat{z}}{\lambda}} \tag{A5}$$

Solving for z:

$$\hat{z} = -\frac{2\lambda}{\pi}\left\{\log(\sqrt{s} + \sqrt{s-1}) + \left(\frac{\lambda-1}{2\lambda}\right)\log s\right\} \tag{A6}$$

using:

$$\frac{dz}{dw} = \frac{1}{q}\, e^{i\theta}$$

$$= (-\pi s)\,\frac{dz}{ds} \tag{A7}$$

we solve for q and θ:

$$(1-\lambda)\,q = \tilde{q} = \sqrt{\frac{1-s}{1+s\phi}}$$

$$\tilde{\theta} = \cos^{-1}\tilde{q} \tag{A8}$$

$$\phi = \frac{2\lambda-1}{(1-\lambda)^2}$$

We now wish to verify the solution by direct substitution into (2-19) that is, show (A8) satisfies:

$$\log\tilde{q} = -\frac{s}{\pi}\,\fint_0^1 \frac{\tilde{\theta}(s')}{s'(s'-s)}\,ds'$$

$$-\frac{s}{\pi}\,\fint_0^1 \frac{\tilde{\theta}(s')}{s'(s'-s)}\,ds' = -\frac{1}{\pi}\log\left|\frac{s'-s}{s'}\right|\tilde{\theta}(s')\Big|_{s'=0}^{s'=1} + \frac{1}{\pi}\,\fint_0^1 \log\left|\frac{s'-s}{s'}\right|\frac{d\tilde{\theta}}{ds}\,ds'$$

$$= \frac{1}{2}\log(1-s) - \frac{\sqrt{1+\phi}}{2\pi}\,\fint_0^1 \log\left|\frac{s'-s}{s'}\right|\frac{1}{\sqrt{s'(1-s')}}\,\frac{ds'}{1+s'\phi} \tag{A9}$$

The principle-value integral on the right can be evaluated by considering the following contour integral:

$$\int_c \log\left(\frac{s'-s}{s'}\right) \frac{1}{s'-a} \frac{1}{\sqrt{s'(1-s')}}\, ds'$$

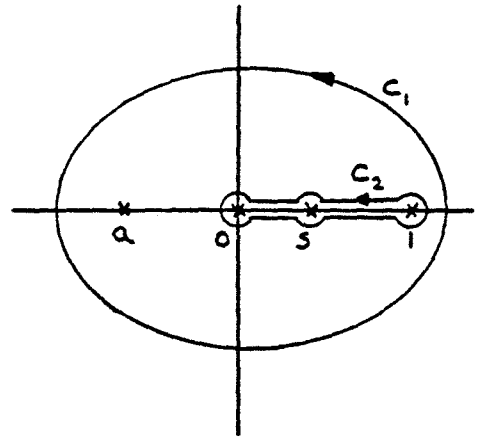

$$\int_{C_1} \to 0 \quad \text{as} \quad R \to \infty$$

$$2\pi i(\text{Residue at a}) + \int_{C_2} = 0 \qquad \text{(A10)}$$

By defining the proper branches along C_2, the real part of (A10) gives:

$$\mathcal{P}\int_0^1 \log\left|\frac{s'-s}{s'}\right| \frac{1}{s'-a} \frac{1}{\sqrt{s'(1-s')}}\, ds' = \pi \log\left|\frac{a-s}{a}\right| \cdot |a(1-a)|^{-1/2} \qquad \text{(A11)}$$

$\therefore$ $$\log \tilde{q} = \frac{1}{2}\log(1-s) - \frac{1}{2}\log(1+s\phi)$$

$$\tilde{q} = \sqrt{\frac{1-s}{1+s\phi}}$$

Thus, (A8) is shown to be a solution of (2-19) for T = 0.

APPENDIX B

To examine the solution of (2-19) near s = 1, we make the change of variables:

$$t = 1 - s \tag{B1}$$

The equations become:

$$q = kq(1-t)\frac{d}{dt}\left(q(1-t)\frac{d\theta}{dt}\right) + \cos\theta \tag{B2a}$$

$$\log q = \frac{1}{\pi} \mathcal{P}\int_0^1 \frac{\theta(t')}{t'-t}\, dt' + A \tag{B2b}$$

$$A = \frac{1}{\pi}\int_0^1 \frac{\theta(t')}{1-t'}\, dt' \tag{B2c}$$

The solution of (B2) for k = 0 may be expanded in a series in $\sqrt{t}$, so we try an expansion of the form (B3) for nonzero k.

$$\begin{aligned} \theta(t) &= -\frac{\pi}{2} + a_1\sqrt{t} + a_2 t + \cdots \\ q(t) &= b_1\sqrt{t} + b_2 t + \cdots \end{aligned} \tag{B3}$$

This expansion is substituted into (B2b). Expanding the logarithm, we obtain:

$$\log b_1 + \frac{1}{2}\log t + \frac{b_2}{b_1}\sqrt{t} + O(t)$$

$$= \frac{1}{\pi}\int_0^1 \frac{\theta(t') + \frac{\pi}{2}}{t'-t}\,dt' - \frac{1}{2}\log\left(\frac{1-t}{t}\right) + A \qquad \text{(B4)}$$

Taking the limit $t \to 0$ in (B4):

$$\log b_1 = \frac{1}{\pi}\int_0^1 \frac{\theta(t') + \frac{\pi}{2}}{t'}\,dt' + A \qquad \text{(B5)}$$

The coefficient b_1 is determined as a global integral of θ over the entire interval.

The expansion (B3) is inserted into the differential equation (B2a). Equating the constant term, we obtain:

$$a_2 b_1 + \frac{1}{2} b_2 a_1 = 0 \qquad \text{(B6)}$$

Consider the integrand in (B4). Since:

$$\int_0^1 \frac{t'}{t'-t}\,dt' = 1 + t\log\left(\frac{1-t}{t}\right) \qquad \text{(B7)}$$

the expansion of the integral will include terms of the form $t^n \log t$. Since these terms cannot be matched, their coefficients must be set to zero. Thus:

$$a_2 = a_4 = \cdots = 0 \qquad \text{(B8)}$$

Using this result in (B2a) shows that the expansion of q does not contain any integral powers of t:

$$b_2 = b_4 = \cdots = 0 \tag{B9}$$

Thus, (B6) is satisfied identically.

At each subsequent stage in the expansion, the differential equation (B2a) specifies a relation between the coefficients $\{a_i, b_i\}$ (e.g., (B6)), while the integral equation (B2b) gives integral conditions on the $\{b_i\}$ (e.g., (B5)). The expansion (B3) appears to be consistent and terms can be matched to high order.

APPENDIX C

The second term in the perturbation expansion of $\theta(s)$ is:

$$\theta_1(s) = \frac{f(s)g(s)}{f^2+\pi^2} + \frac{e^{w(s)}}{\sqrt{f^2+\pi^2}} \int_0^1 \frac{g(s')}{s'-s} \frac{e^{-w(s')}}{\sqrt{f^2+\pi^2}}\, ds' + c\, \frac{e^{w(s)}}{(1-s)\sqrt{f^2+\pi^2}} \qquad (C1)$$

where $f(s)$, $g(s)$ and $w(s)$ are given by (5-4) and (5-5). We now evaluate these terms:

$$\frac{1}{2\pi i} \ln\left(\frac{f(t)+\pi i}{f(t)-\pi i}\right) = \frac{1}{2\pi i} \ln\left(\frac{\tan\theta_0 + i}{\tan\theta_0 - i}\right)$$

$$= \frac{1}{2\pi i}\left(\pi i + 2n\pi i - 2i\theta_0\right)$$

$$= \frac{1}{2} - \frac{\theta_0}{\pi} \qquad (C2)$$

where n has been chosen to satisfy (5-6).

$$w(s) = \int_0^1 \frac{1}{s'-s}\left\{\frac{1}{2} - \frac{\theta_0}{\pi}\right\} ds'$$

$$= \frac{1}{2}\log\left(\frac{1-s}{s}\right) - \frac{s}{\pi}\int_0^1 \frac{\theta_0(s')}{s'(s'-s)}\, ds' - \frac{1}{\pi}\int_0^1 \frac{\theta_0(s')}{s'}\, ds'$$

$$= \frac{1}{2}\log\left(\frac{1-s}{s}\right) + \log q_0 - \log(1-\lambda)$$

$$\therefore \quad e^{w(s)} = \frac{q_0}{1-\lambda}\sqrt{\frac{1-s}{s}} \qquad (C3)$$

Evaluating g(s):

$$g(s) = -\frac{\pi}{4}\sqrt{1+\phi}\,\frac{\sqrt{s}}{(1+s\phi)^{5/2}}(1-2s\phi) - A \qquad (C4)$$

$$\therefore \quad \fint_0^1 \frac{g(s')}{s'-s}\frac{e^{-w(s')}}{\sqrt{f^2+\pi^2}} = \frac{1-\lambda}{\pi}\fint_0^1 \frac{g(s')}{s'-s}\sqrt{\frac{s'}{1-s'}}\,ds'$$

$$= -\frac{(1-\lambda)}{\pi}A\fint_0^1 \frac{1}{s'-s}\sqrt{\frac{s'}{1-s'}}\,ds'$$

$$-\frac{(1-\lambda)}{4}\sqrt{1+\phi}\fint_0^1 \frac{s'}{(1+s'\phi)^{5/2}}\frac{(1-2s'\phi)}{s'-s}\frac{1}{\sqrt{1-s'}}\,ds' \qquad (C5)$$

The first integral in (C5) may be evaluated by considering the contour integral:

$$\int_c \frac{1}{s'-s}\sqrt{\frac{s'}{1-s'}}\,ds'$$

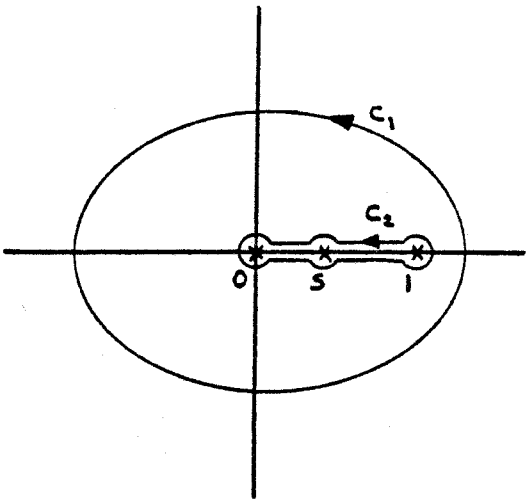

$$\int_{c_1}(\quad)ds' = 2\pi = \int_{c_2}(\quad)ds'$$

By parameterizing the path c_2, we obtain:

$$\fint_0^1 \frac{1}{s'-s}\sqrt{\frac{s'}{1-s'}}\,ds' = \pi \qquad (C6)$$

The second integral in (C5) is more difficult. We write:

$$\fint_0^1 \left(\frac{s'}{s'-s}\right) \frac{1-2s'\phi}{(s'+1/\phi)^{5/2}} \frac{ds'}{\sqrt{1-s'}} = \frac{1}{(s+1/\phi)^2} \fint_0^1 \frac{s'}{s'-s} \frac{1-2s'\phi}{\sqrt{(s'+1/\phi)(1-s')}}\, ds'$$

$$- \frac{1}{(s+1/\phi)^2} \int_0^1 \frac{s'(1-2s'\phi)}{(s'+1/\phi)^{3/2}\sqrt{1-s'}}\, ds' - \frac{1}{s+1/\phi} \int_0^1 \frac{s'(1-2s'\phi)}{(s'+1/\phi)^{5/2}\sqrt{1-s'}}\, ds' \quad (C7)$$

In the first integral of (C7) we change variables to: $t = s'-s$. In the second and third integrals, we let $t = s' + 1/\phi$. In both cases we are left with integrals of the form:

$$\int_a^b \frac{(\text{polynomial in } t)}{t^m \sqrt{\text{quadratic in } t}}\, dt \quad (C8)$$

This integral can be evaluated (laboriously) by indefinite integration. After considerable algebraic manipulation, we obtain:

$$\fint_0^1 \left(\frac{s'}{s'-s}\right) \frac{1-2s'\phi}{(s'+1/\phi)^{5/2}} \frac{1}{\sqrt{1-s'}}\, ds' = \frac{1}{(s+1/\phi)^2} \left\{ \frac{2\sqrt{\phi}}{(\phi+1)^2} \left(1-\phi-2s\phi(2\phi+1)\right) \right.$$

$$\left. + \frac{s(2\phi s-1)}{\sqrt{(s+1/\phi)(1-s)}} \log\left(\frac{s(1+\phi)}{2\sqrt{(1-s)(1+\phi s)} + (\phi-1)s+2} \right) \right\} \quad (C9)$$

Combining all the terms into (C1), we have:

$$\theta_1(s) = q_0 \sin\theta_0 \left(-\frac{\sqrt{1+\phi}}{4} \frac{\sqrt{s}}{(1+s\phi)^{5/2}} (1-2s\phi) - \frac{A}{\pi} \right)$$

$$+ \frac{q_0^2}{\pi(1-\lambda)} \sqrt{\frac{1-s}{s}} \left\{ -(1-\lambda)A - \frac{(1-\lambda)}{4} \frac{\sqrt{1+\phi}}{(1+s\phi)^2} \left[\frac{2}{(\phi+1)^2} \left(1-\phi-2s\phi(2\phi+1)\right) \right.\right.$$

$$\left.\left. + \frac{s(2\phi s-1)}{\sqrt{(1+\phi s)(1-s)}} \log\left(\frac{s(1+\phi)}{2\sqrt{(1-s)(1+\phi s)} + (\phi-1)s+2} \right) \right] \right\}$$

$$+ \frac{c}{(1-\lambda)\pi} \left(\frac{1}{1+s\phi}\right) \sqrt{\frac{1-s}{s}} \quad (C-10)$$

The constant c is chosen to cancel the $1/\sqrt{s}$ singularily at the origin. Finally:

$$\theta_1(s) = \frac{\sqrt{1+\phi}}{\pi}\,\frac{\sqrt{s(1-s)}}{1+s\phi}\left\{A\left(1+\frac{1}{\sqrt{\phi+1}}\right)+\frac{\pi\sqrt{1+\phi}}{4}\,\frac{\sqrt{s}}{(1+s\phi)^{5/2}}(1-2s\phi)\right.$$

$$\left.+\frac{1}{2(1+s\phi)^2}\left[\frac{1+2\phi-s\phi(\phi+2)}{\phi+1}-\frac{\sqrt{1-s}(2\phi s-1)}{2\sqrt{1+\phi s}}\log\left(\frac{s(1+\phi)}{2\sqrt{(1-s)(1+\phi s)}+(\phi-1)s+2}\right)\right]\right\} \qquad \text{(C-11)}$$

APPENDIX D

The change in area due to the perturbation is:

$$A = \int_f^a \delta \, ds \tag{D1}$$

where δ is the normal displacement due to the perturbation, and ds is an element of arc length. There will be an extra flux of fluid proportional to:

$$A_t = \int_f^a \delta_t \, ds \tag{D2}$$

We define γ to be the angle of the normal with the horizontal. The normal displacement δ is:

$$\delta = (\delta x) \cos\gamma + (\delta y) \sin\gamma \tag{D3}$$

where (δx) and (δy) are the horizontal and vertical displacements due to the perturbations. The interface is:

$$x(\phi, \varepsilon F) = x_0(\phi, 0) + \varepsilon F \frac{\partial x_0}{\partial \psi}(\phi, 0) + \varepsilon \xi(\phi, 0) + O(\varepsilon^2)$$

$$y(\phi, \varepsilon F) = y_0(\phi, 0) + \varepsilon F \frac{\partial y_0}{\partial \psi}(\phi, 0) + \varepsilon \eta(\phi, 0) + O(\varepsilon^2)$$

$$\Rightarrow \quad \delta x = \varepsilon \left(F \frac{\partial x_0}{\partial \psi}(\phi, 0) + \xi(\phi, 0) \right) + O(\varepsilon^2)$$

$$\delta y = \varepsilon \left(F \frac{\partial y_0}{\partial \psi}(\phi, 0) + \eta(\phi, 0) \right) + O(\varepsilon^2) \tag{D4}$$

Using the transformation (2-13) we have:

$$\frac{\partial x_0}{\partial \psi} = -\frac{\cos\gamma}{q}$$

$$\frac{\partial y_0}{\partial \psi} = -\frac{\sin\gamma}{q} \tag{D5}$$

Thus, the normal displacement is:

$$\delta = \varepsilon\left(\xi\cos\gamma + \eta\sin\gamma - \frac{F}{q}\right) + O(\varepsilon^2) \tag{D6}$$

The kinematic condition (7-9) is written in terms of the angle γ:

$$F_t + q^2 F_\phi - q\cos\gamma\,\xi_t - q\sin\gamma\,\eta_t = 0 \tag{D7}$$

Thus, we have:

$$\delta_t = \varepsilon q F_\phi \tag{D8}$$

$$\Rightarrow \qquad A_t = \varepsilon\int_f^a qF_\phi\,ds$$

$$= \varepsilon\int_f^a qF_\phi\,\frac{d\phi}{q}$$

$$= \varepsilon F(a) - \varepsilon F(f) \tag{D9}$$

For an antisymmetric perturbation, F is even, so A_t vanishes immediately. For a symmetric perturbation, equation (7-30) implies $W = 0$ at the endpoints. Thus:

$$F(a) = F(f) = 0$$

$$\Rightarrow \qquad A_t = 0 \tag{D10}$$

In both the symmetric and antisymmetric cases, there is no extra flux from the perturbations.

REFERENCES

G. F. Carrier, M. Krook, and C. E. Pearson, Functions of a Complex Variable, McGraw-Hill (1966)

G. D. Crapper, An Exact Solution for Progressive Capillary Waves of Arbitrary Amplitude, J. Fluid Mech. 2 (1957), pp. 532-540

H. Darcy, Les Fontaines, Publiques de Ville de Dijon, Paris (1856)

H. J. S. Hele-Shaw, On the Motion of a Viscous Fluid Between Two Parallel Plates, Nature 58 (1898)

H. Lamb, Hydrodynamics, Sixth Edition, Dover (1932)

M. S. Longuet-Higgins, The Instabilities of Gravity Waves of Finite Amplitude in Deep Water, Proc. R. Soc. Land. A 360 (1978), pp. 971-488

E. Pitts, Penetration of Fluid into a Hele-Shaw Cell, J. Fluid Mech. 97 (1980), pp. 53-64

P. G. Saffman and G. I. Taylor, The Penetration of a Fluid Into a Porous Medium or Hele-Shaw Cell, Proc. Roy. Soc. A 245 (1958), pp. 312-329

G. I. Taylor, Deposition of a Viscous Fluid on the Wall of a Tube, J. Fluid Mech. 10 (1961), pp. 161-165

_____, The Instability of Liquid Surfaces When Accelerated in a Direction Perpendicular to Their Planes, Proc. Roy. Soc. A 201 (1950), pp. 192-196

G. I. Taylor and P. G. Saffman, Cavity Flows of Viscous Fluids in Narrow Spaces, Second Symposium on Naval Hydrodynamics, (1958)

M. Van Dyke, Perturbation Methods in Fluid Mechanics, Parabolic Press, (1975)

R. A. Wooding and H. J. Morel-Seytoux, Multiphase Fluid Flow Through Porous Media, Ann. Rev. Fluid. Mech (1976)

Part II

THE KINETIC EQUATION FOR HAMILTONIAN SYSTEMS

1. INTRODUCTION

A statistical description of nonlinear wave fields is appropriate for a variety of physical problems (ocean waves, plasma turbulence, etc.). For linear waves, the component Fourier wave amplitudes are uncoupled. We will be interested in the weak nonlinear interactions of the wave amplitudes, which gives rise to a slow variation of the wave amplitudes.

We assume the nonlinearities have an expansion in powers of the amplitude. The equations of motion will have the form:

$$\frac{\partial a(k,t)}{\partial t} - i\omega(k)\, a(k,t) = Aa^2 + Ba^3 + Ca^4 + Da^5 + \cdots \qquad (1\text{-}1)$$

The amplitudes $a(k,t)$ are taken to be random variables.

The quantity of interest is the correlation of the wave amplitudes, corresponding to the energy spectrum function. Since we assume the amplitudes are small, details about the wave field may be obtained by perturbation methods (e.g., Benney and Saffman 1966 , Hasselmann 1967).

Our interest will be in the equation for the time evolution of the energy spectrum function. This equation, often called the kinetic equation, has been obtained by a number of authors (Benney and Saffman 1966 , Hasselmann 1967, Zakharov 1967), and takes the forms

$$\frac{\partial n(k,t)}{\partial t} = \int\int S n_{k_1} n_{k_2} \delta(k \pm k_1 \pm k_2)\ \delta(\omega \pm \omega_1 \pm \omega_2)\, dk_1 dk_2$$

$$+ \int\int\int T\, n_{k_1} n_{k_2} n_{k_3} \delta(k \pm k_1 \pm k_2 \pm k_3)\ \delta(\omega \pm \omega_1 \pm \omega_2 \pm \omega_3) dk_1 dk_2 dk_3$$

$$+ \text{higher order terms} \qquad (1\text{-}2)$$

where:

$$\langle a_k\, a^*_{k'} \rangle = \delta(k-k') n_k$$

$$\omega_1 = \omega(k_1)$$

$$a_k = a(k,t) \qquad \text{etc.}$$

$$S = S(k, k_1, k_2) \text{ etc.}$$

n_k is the energy spectrum function. The coefficients S and T are called the interaction coefficients.

If the dispersion relation allows resonance among three wave numbers, the dominant contribution in the kinetic equation is of order $(a_k)^4$. For many problems however, resonance cannot occur with three wave numbers (e.g., gravity waves, see Phillips 1960). In this case, the first term in the kinetic equation vanishes, and the dominant contribution comes from the next term, of order $(a_k)^6$.

The interaction coefficients S and T depend upon the nonlinear coefficients, A, B, C, D in the expansion (1-1). In particular, the coefficient S must account for all interactions between four wave

amplitudes. An inspection of the perturbation expansion shows that the first two terms in (1-1), corresponding to coefficients A and B, contribute at this order. Similarly, the coefficient T accounts for interactions between 6 waves, and formally will depend upon A, B, C, and D.

Most authors restrict their attention to quadratic nonlinearities, that is, they take $B = C = D = 0$ in the equations of motion (1-1). Even in the first term of the kinetic equation, the neglect of the cubic term is an inconsistency in the perturbation expansion.

A few authors have kept the higher order nonlinearities. Although they begin with an expansion of the form (1-1), the kinetic equation they present is missing contributions from the quartic and quintic terms (e.g., Hasselmann 1966). It is not clear at what point in the analysis these terms are dropped.

Our objective is to understand why the missing terms do not appear in the kinetic equation, and to confirm the given equations. The equations of motion are stated in a very general Hamiltonian form. The analysis of the resulting perturbation expansion is facilitated with the use of Wyld diagrams (Wyld 1961). The results obtained here differ from those reported in the literature. It is shown that the higher order nonlinearities do contribute to the kinetic equation, but they do not contribute at leading order.

2. FORMULATION OF THE PROBLEM

Although the equations of motion in "natural" variables (pressure, velocity, etc.) are usually not Hamiltonian equations, it is often possible to cast the equations in a Hamiltonian form (Zakharov 1967, 1968). We therefore use a general Hamiltonian system to describe the motion. We will follow the notation of Zakharov (1974, 1975).

The motion is described by the generalized coordinate $q(x, t)$, and the generalized momentum $p(x, t)$. For simplicity, we consider the problem in one space dimension. The equations of motion are:

$$\frac{\partial q}{\partial t} = \frac{\delta H}{\delta p} \qquad \frac{\partial p}{\partial t} = -\frac{\delta H}{\delta q} \tag{2-1}$$

where the Hamiltonian H is expanded in powers of p and q.

$$H = H_0 + H_{int}$$

The first term in the expansion H_0 will be quadratic in p and q. H_{int} will contain all higher order terms.

For a spatially homogeneous medium, H_0 takes the form:

$$H_0 = \frac{1}{2} \int \Big\{ U(x-x')\, p(x)\, p(x') + 2V(x-x')\, p(x)\, q(x') + W(x-x')\, q(x)\, q(x') \Big\}\, dx\, dx' \tag{2-2}$$

$$U(x) = U(-x)$$

$$W(x) = W(-x)$$

If we assume the medium is invariant to reflection of coordinates, the coefficient V is symmetric:

$$V(-x) = V(x)$$

Performing a Fourier transform:

$$p_k = \frac{1}{\sqrt{2\pi}} \int_{-\infty}^{\infty} p(x)\, e^{-ikx}\, dx \qquad p_{-k} = p_k^*$$

$$p(x) = \frac{1}{\sqrt{2\pi}} \int_{-\infty}^{\infty} p_k\, e^{ikx}\, dk$$

we have:

$$H_0 = \frac{1}{2} \int \left\{ U_k p_k p_k^* + 2V_k p_k q_k^* + W_k q_k q_k^* \right\} dk \qquad (2\text{-}3)$$

where:

$$U_k = \frac{1}{\sqrt{2\pi}} \int_{-\infty}^{\infty} U(x) e^{-ikx}\, dx \qquad U_{-k} = U_k = U_k^*$$

etc.

The equations of motion take the form:

$$\frac{\partial p_k}{\partial t} = -\frac{\delta H}{\delta q_k^*} \qquad \frac{\partial q_k}{\partial t} = \frac{\delta H}{\delta p_k^*} \qquad (2\text{-}4)$$

We perform a change of variables that reduces the equations of motion to a single equation. Define:

$$a_k = \alpha_k p_k + \beta_k q_k \qquad \alpha_{-k} = \alpha_k$$

$$a_k^* = \alpha_k^* p_k^* + \beta_k^* q_k^* \qquad \beta_{-k} = \beta_k$$

$$\alpha_k \beta_k^* - \alpha_k^* \beta_k = i$$

The equations of motion become:

$$\frac{\partial a_k}{\partial t} + i \frac{\delta H}{\delta a_k^*} = 0 \tag{2-5}$$

The coefficients α_k and β_k are chosen to diagonalize the leading term H_0. We restrict our attention to the case where the equation of motion admit travelling wave solutions. For travelling waves to exist, it is necessary that:

$$U_k W_k > V_k^2$$

For simplicity, we take U_k and W_k to both be positive. The coefficients α_k, β_k are chosen to be:

$$\alpha_k = \sqrt{\frac{U_k}{2\omega_k}} \qquad \beta_k = \sqrt{\frac{1}{2U_k\omega_k}}\,(V_k + i\omega_k)$$

$$\omega_k = \sqrt{U_k W_k - V_k^2} \qquad \omega_k = \omega_{-k}$$

The choice gives:

$$H_0 = \int \omega_k a_k a_k^* \, dk \tag{2-6}$$

Neglecting H_{int}, the nonlinear term in the equations of motion, the linear solution is:

$$a_k^s = (\text{constant}) \cdot e^{-is\omega_k t}$$

where:

$$a_k,\ a_k^* = a_k^s \qquad s = \pm 1$$

This we will call a "free" wave. The effect of the nonlinear terms is to cause a slow variation in the amplitudes of the "free" waves. We now expand the nonlinear term H_{int} in a power series in the wave amplitude:

$$H_{int} = \frac{1}{3} \int \sum_{s_1 s_2 s_3} A_{k_1 k_2 k_3}^{s_1 s_2 s_3} a_{k_1}^{s_1} a_{k_2}^{s_2} a_{k_3}^{s_3} \delta\left(s_1 k_1 + s_2 k_2 + s_3 k_3\right) dk_1 dk_2 dk_3$$

$$+\frac{1}{4} \int \sum_{s_1 - s_4} B_{k_1 - k_4}^{s_1 - s_4} a_{k_1}^{s_1} - a_{k_4}^{s_4} \delta\left(s_1 k_1 + \cdots + s_4 k_4\right) dk_1 - dk_4$$

$$+\frac{1}{5} \int \sum_{s_1 - s_5} C_{k_1 - k_5}^{s_1 - s_5} a_{k_1}^{s_1} - a_{k_5}^{s_5} \delta\left(s_1 k_1 + \cdots + s_5 k_5\right) dk_1 - dk_5$$

$$+\frac{1}{6} \int \sum_{s_1 - s_6} D_{k_1 - k_6}^{s_1 - s_6} a_{k_1}^{s_1} - a_{k_6}^{s_6} \delta\left(s_1 k_1 + \cdots + s_6 k_6\right) dk_1 - dk_6$$

$$+ \text{higher order terms} \qquad (2\text{-}7)$$

Since H is real:

$$\left(A^{s_1 s_2 s_3}_{k_1 k_2 k_3}\right)^* = A^{-s_1 -s_2 -s_3}_{k_1 k_2 k_3} \qquad \text{etc.}$$

The coefficients also have permutation symmetry:

$$A^{s_1 s_2 s_3}_{k_1 k_2 k_3} = A^{s_2 s_1 s_3}_{k_2 k_1 k_3} = A^{s_3 s_2 s_1}_{k_3 k_2 k_1} \qquad \text{etc.}$$

The equations of motion (2-5) become:

$$\begin{aligned} i s \frac{\partial a^s_k}{\partial t} - \omega_k a^s_k &= \int \sum_{s_1 s_2} A^{-s s_1 s_2}_{k k_1 k_2} a^{s_1}_{k_1} a^{s_2}_{k_2} \delta\left(-sk + s_1 k_1 + s_2 k_2\right) dk_1 dk_2 \\ &+ \int \sum_{s_1 - s_3} B^{-s s_1 - s_3}_{k k_1 - k_3} a^{s_1}_{k_1} - a^{s_3}_{k_3} \delta\left(-sk + s_1 k_1 + \cdots + s_3 k_3\right) dk_1 - dk_3 \\ &+ \int \sum_{s_1 - s_4} C \\ &+ \int \sum_{s_1 - s_5} D \\ &+ \text{higher order terms} \end{aligned} \qquad (2\text{-}8)$$

To simplify the notation, we make the following definitions:

$$C_k^s \equiv a_k^s \, e^{i s \omega_k t}$$

$$\omega_1 \equiv \omega_{k_1}$$

$$A^{-++}_{k_{12}}(t) \equiv A_{k k_1 k_2}^{-s s_1 s_2} \, e^{-i(-s\omega + s_1\omega_1 + s_2\omega_2)t} \tag{2-9}$$

We expect the nonlinear interactions to cause a slow variation in the C_k^s. Equation (2-8) becomes:

$$\frac{\partial C_k^s}{\partial t} = -is \int \sum_{s_1 s_2} A^{-++}_{k_{12}}(t) \, C_{k_1}^{s_1} C_{k_2}^{s_2} \, \delta\left(-sk + s_1 k_1 + s_2 k_2\right) dk_1 dk_2$$

$$-is \int \sum_{s_1 - s_3} B^{-+++}_{k_{123}}(t) C_{k_1}^{s_1} - C_{k_3}^{s_3} \, \delta\left(-sk + s_1 k_1 + \cdots + s_3 k_3\right) dk_1 - dk_3$$

$$-is \int \sum \; C$$

$$-is \int \sum \; D$$

$$+ \text{ higher order terms} \tag{2-10}$$

3. THE PERTURBATION EXPANSION

The solution is developed as a perturbation expansion in the amplitude:

$$C_k^s = {}_1C_k^s + {}_2C_k^s + {}_3C_k^s + \cdots \tag{3-1}$$

where:

$${}_nC_k^s = O(\varepsilon^n) \qquad 0 < \varepsilon << 1$$

ε = characteristic amplitude

We write out the equations for the perturbations:

$$\frac{\partial {}_1C_k^s}{\partial t} = 0$$

$$\frac{\partial {}_2C_k^s}{\partial t} = -is\int \sum_{s_1 s_2} A_{k12}^{-++}(t)\, {}_1C_{k_1}^{s_1}\, {}_2C_{k_2}^{s_2}\, \delta\left(-sk + s_1k_1 + s_2k_2\right) dk_1 dk_2$$

$$\frac{\partial {}_3C_k^s}{\partial t} = -is\int \sum_{s_1 s_2} A_{k12}^{-++}(t)\left({}_1C_{k_1}^{s_1}\, {}_2C_{k_2}^{s_2} + {}_2C_{k_1}^{s_1}\, {}_1C_{k_2}^{s_2}\right)\delta\left(-sk + s_1k_1 + s_2k_2\right) dk_1 dk_2$$

$$-is\int \sum_{s_1 - s_3} B_{k123}^{-+++}(t)\, {}_1C_{k_1}^{s_1} - {}_1C_{k_3}^{s_3}\, \delta\left(-sk + s_1k_1 + \cdots + s_3k_3\right) dk_1 - dk_3$$

etc. (3-2)

Since ${}_1C_k^s$ is independent of time, the only time dependence for ${}_2C_k^s$ comes in through the coefficient A(t). We integrate the equations to obtain:

$$ {}_1C_k^s = \text{constant} $$

$$ {}_2C_k^s = -is \int \sum_{s_1 s_2} \left(\int_0^t A_{k12}^{-++}(t')dt' \right) {}_1C_{k_1}^{s_1} \, {}_1C_{k_2}^{s_2} \delta\left(-sk+s_1k_1+s_2k_2\right) dk_1 dk_2 $$

$$ {}_3C_k^s = -2is \int \sum_{s_1 s_2} \left(\int_0^t A_{k12}^{-++}(t') \, {}_2C_{k_2}^{s_2}(t')dt' \right) {}_1C_{k_1}^{s_1} \delta\left(-sk+s_1k_1+s_2k_2\right) dk_1 dk_2 $$

$$ -is \int \sum_{s_1 - s_3} \left(\int_0^t B_{k123}^{-+++}(t')dt' \right) {}_1C_{k_1}^{s_1} - {}_1C_{k_3}^{s_3} \delta\left(-sk+s_1k_1+\cdots+s_3k_3\right) dk_1 - dk_3 $$

etc. (3-3)

Clearly, to carry out this perturbation expansion to higher order would be difficult if not impossible as it stands. In order to proceed, we introduce Wyld diagrams to manipulate the perturbation expansion (Wyld 1961). The idea is to make a one-to-one correspondence between terms of the perturbation series and a set of diagrams. We make the following correspondence:

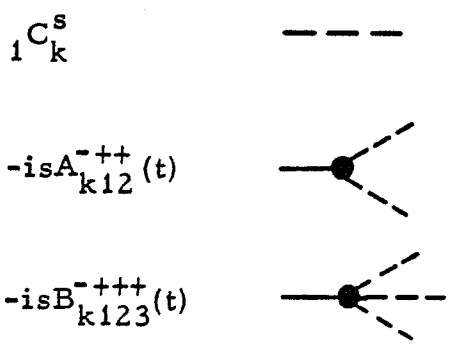

etc.

Each "vertex" represents a coefficient A, B, C, etc., which is distinguished by the number of "branches" leaving the vertex. At each vertex, we multiply by the appropriate delta function, sum over the indices s_1, s_2 etc., and integrate over the appropriate dummy variables k_1, k_2 etc. A solid line indicates time integration. Thus (3-3) is represented by:

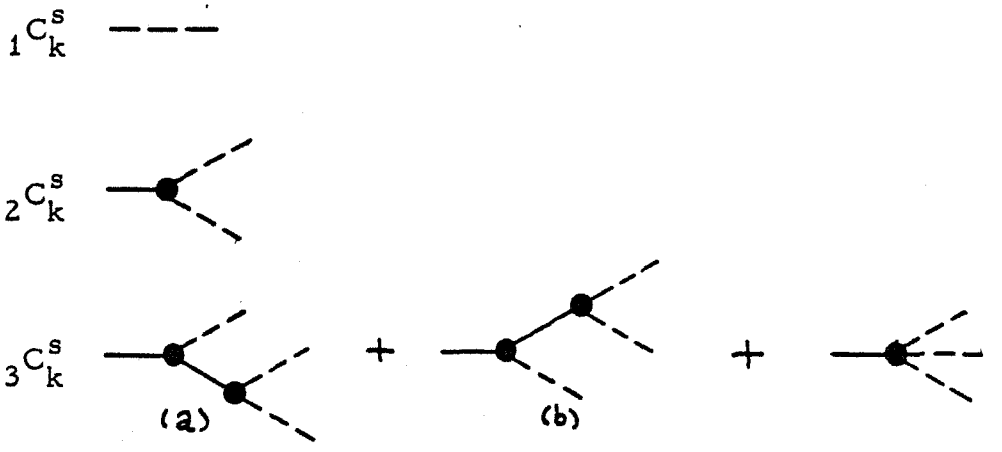

Diagrams (a) and (b) correspond to the same integral (compare (3-2) and (3-3)) and may be combined. Thus, we have an additional factor with each "combined" diagram corresponding to the number of "simple" diagrams which are topologically equivalent. Finally:

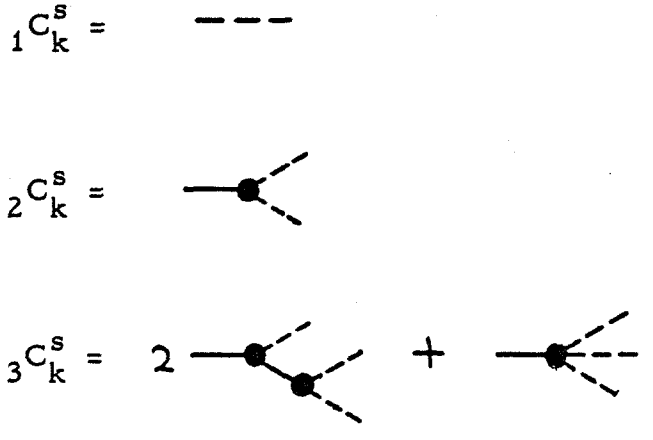

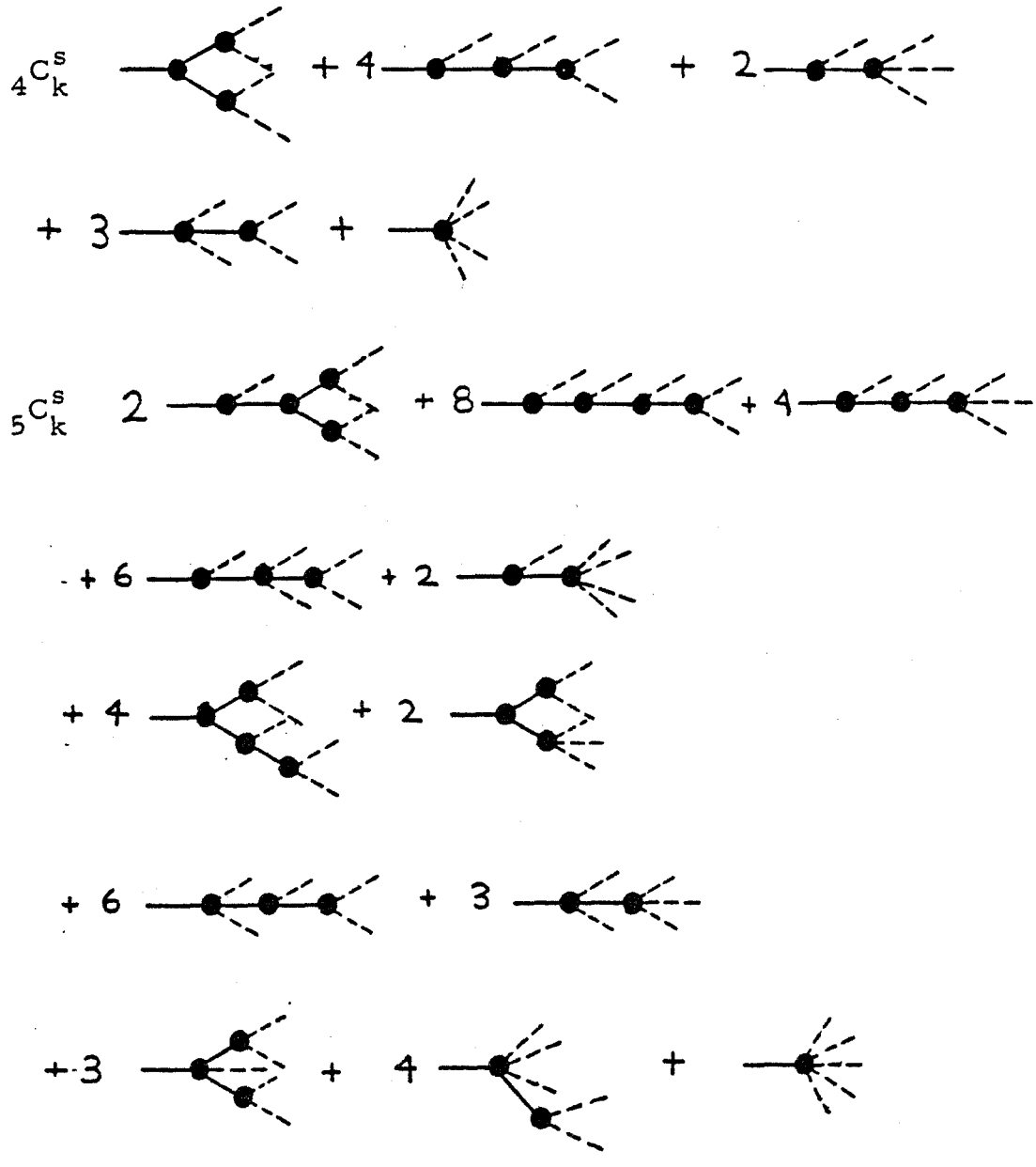

The diagrams for ${}_nC_k^s$ consist of all topologically different "trees" which branch with n free wave components. In all cases, it is possible (but tedious!) to write out the analytic expansion for the ${}_nC_k^s$ and compare with the diagrams.

We now obtain an expression for the energy spectrum. The momentum $p(x, t)$ is assumed to be a stationary random function of

position. The two point correlation function is defined as:

$$R(r, t) = \langle p(x + r, t)\, p(x, t) \rangle \tag{3-4}$$

where: $\langle \cdot \rangle$ denotes probability averaging.

Taking the Fourier transform, the energy spectrum function is obtained:

$$\psi(k, t) = \frac{1}{\sqrt{2\pi}} \int_{-\infty}^{\infty} R(r, t)\, e^{-ikr}\, dr$$

$$\langle p(k, t)\, p(k', t) \rangle = \delta(k+k')\ \psi(k, t) \tag{3-5}$$

Writing in terms of C_k^s :

$$\langle C_k^s(t)\, C_{k'}^{s'}(t) \rangle = n_k(t)\ \delta(k-k')\ \delta_s \tag{3-6}$$

where:

$$n_k(t) = \frac{W_k}{2\omega_k}\ \psi(k, t)$$

$\delta(k-k')$ is the Dirac delta function

$$\delta_{s,-s'} = \begin{cases} 1 & \text{if } s = -s' \\ 0 & \text{otherwise} \end{cases}$$

The usual way to obtain the kinetic equation is to multiply the equation for C_k^s (eq. (2-10)) by $C_{k_1}^{s_1}$ and average. The resulting

expression for n_k contains correlations of three or more wave amplitudes, and the system of equations is not closed. Although it is unnecessary to do so, most authors make a statistical assumption at this point to close the equations (Benney and Saffman 1966). For simplicity, we follow this convention and assume that ${}_1C_k^s$ is gaussian.

Taking ${}_1C_k^s$ to be gaussian with mean zero, products of an odd number of ${}_1C_k^s$ vanish, while even products may be factored pairwise:

$$\langle {}_1C_{k_1}^{s_1} {}_1C_{k_2}^{s_2} {}_1C_{k_3}^{s_3} {}_1C_{k_4}^{s_4} \rangle$$

$$= \langle {}_1C_{k_1}^{s_1} {}_1C_{k_2}^{s_2} \rangle \langle {}_1C_{k_3}^{s_3} {}_1C_{k_4}^{s_4} \rangle + \langle {}_1C_{k_1}^{s_1} {}_1C_{k_3}^{s_3} \rangle \langle {}_1C_{k_2}^{s_2} {}_1C_{k_4}^{s_4} \rangle + \langle {}_1C_{k_1}^{s_1} {}_1C_{k_4}^{s_4} \rangle \langle {}_1C_{k_2}^{s_2} {}_1C_{k_3}^{s_3} \rangle$$

etc. (3-7)

The energy spectrum is expanded:

$$\langle C_k^s C_k^{-s} \rangle = \langle {}_1C_k^s \, {}_1C_k^{-s} \rangle + \langle {}_1C_k^s \, {}_3C_k^{-s} \rangle + \langle {}_2C_k^s \, {}_2C_k^{-s} \rangle + \langle {}_3C_k^s \, {}_1C_k^{-s} \rangle$$

$$+ \langle {}_1C_k^s \, {}_5C_k^{-s} \rangle + \langle {}_2C_k^s \, {}_4C_k^{-s} \rangle + \langle {}_3C_k^s \, {}_3C_k^{-s} \rangle + \langle {}_4C_k^s \, {}_2C_k^{-s} \rangle + \langle {}_5C_k^s \, {}_1C_k^{-s} \rangle$$

+ higher order terms (3-8)

Terms such as $\langle {}_1C_k^s \, {}_2C_k^{-s} \rangle$ are correlations of an odd number of ${}_1C_k^s$ and therefore vanish.

We now compute some of the terms in the expansion. A wavy line will indicate the lowest order correlation:

$$\langle {}_1C_{k_1}^{s_1}\ {}_1C_{k_2}^{s_2}\rangle = {}_1n_{k_1}\,\delta(k_1-k_2)\,\delta_{s_1,-s_2} = \sim\!\!\sim$$

$$= n_1\,\delta_{1-2}$$

where:
$$n_1 \equiv {}_1n_{k_1}$$

$$\delta_{1-2} \equiv \delta(k_1-k_2)\,\delta_{s_1,-s_2}$$

$$\langle {}_2C_{k2}^{s}\,{}_2C_{k'}^{s'}\rangle = -is\int \sum_{s_1 s_2} \int_0^t \bar{A}^{++}_{k12}(t')dt'\ \delta(-sk+1+2)$$

$$\cdot(-is')\int \sum_{s_3 s_4} \int_0^t \bar{A}^{++}_{k'34}(t'')dt''\ \delta(-s'k'+3+4)$$

$$\cdot\langle {}_1C_{k_1}^{s_1}\ {}_1C_{k_2}^{s_2}\ {}_1C_{k_3}^{s_3}\ {}_1C_{k_4}^{s_4}\rangle\, dk_1dk_2dk_3dk_4$$

$$= -ss'\int\int \sum_{s_1-s_4} \int_0^t \int_0^t \bar{A}^{++}_{k12}(t')\bar{A}^{++}_{k'34}(t'')dt'\,dt''$$

$$\cdot\ \delta(-sk+1+2)\,\delta(-s'k'+3+4)\Big\{n_1n_3(\delta_{1-2}\delta_{3-4}+\delta_{1-4}\delta_{2-3})$$

$$+ n_1n_2\,\delta_{1-3}\delta_{2-4}\Big\}\,dk_1-dk_4 \qquad (3\text{-}9)$$

where:
$$\delta(-sk+1+2) = \delta(-sk+s_1k_1+s_2k_2)$$

Diagrammatically:

$$\langle {}_2C^s_k\, {}_2C^{s'}_{k'}\rangle =$$

$$=$$

The first term is:

$$= \left\{ \int \sum_{s_1} \int_0^t A^{-++}_{k11}(t')dt'\, n_{k_1}\, dk_1 \right\}^2 \delta(sk)\ \delta(-sk') \qquad (3\text{-}10)$$

Note that:

$$\langle {}_2C^s_k\rangle = -is \int \sum \int_0^t A^{-++}_{k11}(t')dt'\, n_1\, dk_1\ \delta(sk)$$

We choose the coordinate system such that:

$$\langle C^s_0\rangle = 0$$

With this choice of coordinate system, we have:

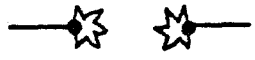

$$= 0$$

The other two integrals combine to give:

$$\langle {}_2C^s_{k2} C^{-s}_{k'}\rangle = 2\delta_{k',k} \int \sum_{s_1 s_2} \left| \int_0^t A^{-++}_{k12}(t')dt' \right|^2 n_1 n_2\ \delta(-sk+1+2)dk_1 dk_2$$

$$= 2$$

(3-11)

Using the fact that $\langle C_0^s \rangle = 0$, and combining topologically equivalent diagrams, we compute more terms:

$\langle {}_3C_{k\,1}^{s}\, C_{k'}^{s'} \rangle = 2$ 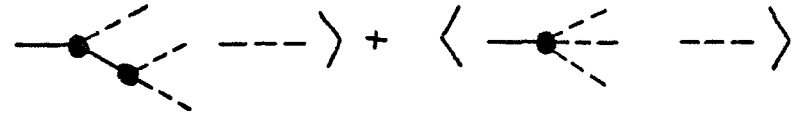 $+$

$=$ $2\{2$ 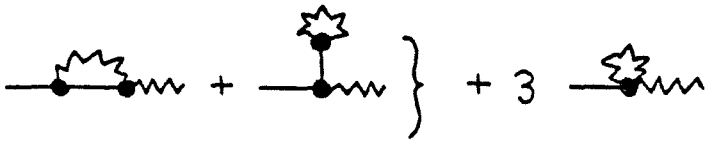 $\}$ $+ 3$

$=$ 4 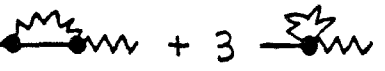 $+ 3$

The term $\langle {}_1C_{k\,3}^{s}\, C_{k'}^{-s} \rangle$ is merely the complex conjugate of $\langle {}_3C_{k\,1}^{s}\, C_{k'}^{-s} \rangle$. The complete expansion is thus:

$\langle C_k^s \, C_{k'}^{-s} \rangle =$  (1)

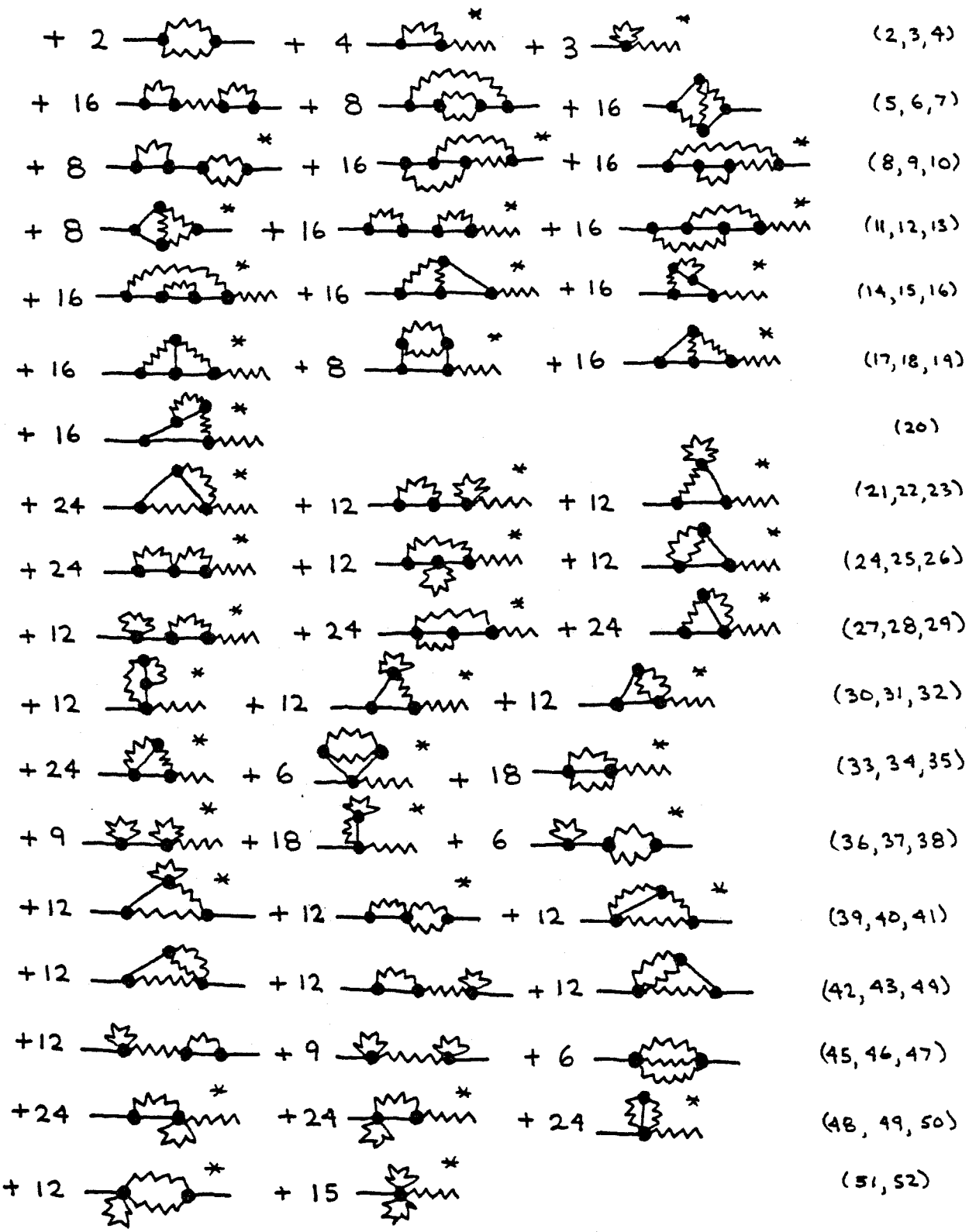

+ complex conjugate of (*) diagrams

+ higher order terms

Note that the order of the terms corresponds to the number of wavy lines in the diagram.

Wyld (1961) considered only quadratic nonlinearities. His perturbation expansion contains only the vertices with two branches, namely diagrams 1, 2, 3, and 5-20. Hasselmann (1966) considered the general case of a power series expansion for the Hamiltonion. The results he presents (without comment as to derivation) are missing terms corresponding to the higher order nonlinearities in the expansion, namely missing terms containing the coefficients C and D. In the diagram picture, vertices with four or five branches are missing in the Hasselmann solution.

Zakharov (1970) uses a different approach. For the case where resonance does not occur with three wave numbers, Zakharov performs a canonical transformation to eliminate the quadratic nonlinearities. Although difficult to compare results, his kinetic equation does not involve the coeffcients C and D.

We focus our attention on those terms not contained in the Hasselmann or Zakharov analysis, namely diagrams 4 and 48-52.

4. ANALYSIS OF THE DIAGRAMS

We are interested in those terms in the perturbation expansion which give rise to a spectral energy flux. Diagram 1 is constant, so we proceed to diagram 2. The time dependence in (3-11) is:

$$\left| \int_0^t A^{-++}_{k12}(t')dt' \right|^2 = \left| A^{-++}_{k12} \right|^2 \left| \int_0^t e^{-i(s\omega+s_1\omega_1+s_2\omega_2)t'} dt' \right|^2$$

$$\frac{d}{dt} \left| \int_0^t e^{-i\omega t'} dt' \right|^2 = e^{i\omega t} \int_0^t e^{-i\omega t} dt + \text{complex conjugate}$$

$$= 2 \frac{\sin \omega t}{\omega} \tag{4-1}$$

The nonlinear interactions produce slow variations in the wave amplitudes. Thus, we will be interested in time scales long compared to the period of the linear wave. Consider:

$$\lim_{t\to\infty} \int_{-\infty}^{\infty} f(\omega') \frac{\sin(\omega-\omega')t}{\omega-\omega'} d\omega'$$

$$= \lim_{t\to\infty} \int_{\omega-a}^{\omega+a} f(\omega') \frac{\sin(\omega-\omega')t}{\omega-\omega'} d\omega' \quad \text{(Rieman-Lebesque lemma)}$$

$$\simeq f(\omega) \lim_{t\to\infty} \int_{\omega-a}^{\omega+a} \frac{\sin(\omega-\omega')t}{\omega-\omega'} d\omega'$$

$$= f(\omega) \lim_{t\to\infty} \int_{-at}^{at} \frac{\sin x}{x} d\omega = \pi f(\omega)$$

We therefore write:

$$\lim_{t\to\infty} \left\{ \frac{\partial}{\partial t} \left| \int_0^t e^{-i\omega t'} dt' \right|^2 \right\} = 2\pi \delta(\omega) \tag{4-2}$$

For diagram 2:

$$\frac{\partial}{\partial t}\left\{ \text{  } \right\} = 2\pi \int \sum_{s_1 s_2} n_1 n_2 \left| A^{-++}_{k12} \right|^2 \delta(-sk+1+2)\, \delta(-s\omega + s_1\omega_1 + s_2\omega_2) dk_1 dk_2 \tag{4-3}$$

Diagram 3

$$\text{  } = -s \int \sum_{s_1 s_2} s_1 \int_0^t A^{-++}_{k12}(t') \int_0^{t'} A^{-++}_{k12}(t'')^* dt'' dt'\, n_k n_2\, \delta(-sk+1+2) dk_1 dk_2$$

$$\frac{\partial}{\partial t}\left\{ \text{  } \right\} \propto \bar{A}^{++}_{k12}(t) \int_0^t A^{-++}_{k12}(t')^*\, dt'$$

Combining this term with its complex conjugate:

$$\frac{\partial}{\partial t}\left\{ \text{  } \right\} = -2\pi s n_k \int \sum_{s_1 s_2} s_1 \left| A^{-++}_{k12} \right|^2 n_1\, \delta(-sk+1+2)\, \delta(-s\omega + s_1\omega_1 + s_2\omega_2) dk_1 dk_2 \tag{4-4}$$

For diagram 4:

$$\text{  } = -isn_k \int \sum_{s_1} B^{-+-+}_{kk11}(t)\, n_1\, dk_1$$

$$B^{-+-+}_{kk11}(t) = B^{-+-+}_{kk11}\, e^{i(-s\omega + s\omega - s_1\omega_1 + s_1\omega_1)t}$$

$$= B^{-+-+}_{kk11}$$

Furthermore:

$$(B^{-+-+}_{kk11})^* = B^{+-+-}_{kk11} = B^{-+-+}_{kk11} = \text{REAL}$$

So term 4 is purely imaginary. Thus:

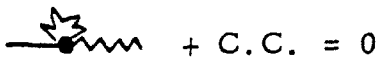 + C.C. = 0

If the dispersion relation allows resonance with three wave numbers, that is, if:

$$-sk + s_1k_1 + s_2k_2 = 0$$
$$-s\omega + s_1\omega_1 + s_2\omega_2 = 0 \qquad (4\text{-}5)$$

has a simultaneous solution, then there is energy transfer at this order. Since $n_k = O(\varepsilon^2)$, the interaction of three waves produces slow variation in n_k of order ε^4.

For many cases of interest (gravity waves in particular), (4-5) does not have a solution, and there is no energy flux of order ε^4. We therefore go to the next order (terms of order ε^6), examining those diagrams not appearing in Hasselmann's (1966) or Zakharov's (1970) analysis.

Diagram 48

$$= -is \int \sum_{s_1 - s_6} \int_0^t A^{-++}_{k12}(t') \int_0^{t'} (-is_1) C^{-++++}_{13456}(t'')dt''dt'\ \delta(-sk+1+2)$$

$$\delta(-s_1 k_1 + 3 + 4 + 5 + 6) n_2 n_4 n_6\ \delta_{2-3}\delta_{4-5}\delta_{6-k'}\, dk_1 - dk_6$$

$$= -sn_k \delta_{k-k'} \int \sum s_1 \int_0^t A^{-++}_{k12}(t') \int_0^{t'} C^{+---+}_{k1244}(t'')dt''dt' n_2 n_4 \delta(-sk+1+2)dk_1 dk_2 dk_4$$

(4-6)

Diagram 49

$$= -is \int \sum_{s_1 - s_6} \int_0^t C^{-++++}_{k1234}(t') \int_0^{t'} (-is_1) A^{-++}_{156}(t'')dt''dt'\ \delta(-sk+1+2+3+4)$$

$$\delta(-s_1 k_1 + 5 + 6) n_2 n_4 n_6\ \delta_{2-5}\delta_{3-4}\delta_{6-k'} dk_1 - dk_6$$

$$= -sn_k \delta_{k-k'} \int \sum s_1 \int_0^t C^{-+++-}_{k1244}(t') \int_0^{t'} A^{+--}_{k12}(t'')dt''dt' n_2 n_4 \delta(-sk+1+2)dk_1 dk_2 dk_4$$

(4-7)

Evaluating the time dependence:

$$\frac{\partial}{\partial t}\{48\} \propto A^{-++}_{k12}(t)\int_0^t C^{+---+}_{k1244}(t')dt'$$

$$= A^{-++}_{k12}\, C^{+---+}_{k1244}\, e^{-i(-s\omega+1+2)t}\int_0^t e^{-i(s\omega-1-2)t'}\, dt'$$

$$= A^{-++}_{k12}\, C^{+---+}_{k1244}\, \frac{1-e^{-i(-s\omega+1+2)}}{-i(s\omega-1-2)}$$

$$\frac{\partial}{\partial t}\{49\} \propto C^{-+++-}_{k1244}(t)\int_0^t A^{+--}_{k12}(t')dt'$$

$$= C^{-+++-}_{k1244}\, A^{+--}_{k12}\, e^{-i(-s\omega+1+2)t}\int_0^t e^{-i(s\omega-1-2)t'}\, dt'$$

$$= C^{-+++-}_{k1244}\, A^{+--}_{k12}\, \frac{1-e^{-i(-s\omega+1+2)t}}{-i(s\omega-1-2)}$$

$$\therefore\ \frac{\partial}{\partial t}\{48 + 49 + C.C.\}$$

$$= -4s n_k \delta_{k-k'} \mathrm{Re}\left\{\int\sum s_1 A^{-++}_{k12}\, C^{+---+}_{k1244}\, n_2 n_4 \delta(-sk+1+2)\frac{\sin(s\omega-1-2)t}{s\omega-1-2}\, dk_1 dk_2\right\}$$

Using (4-2), we have:

$$\lim_{t\to\infty}\frac{\partial}{\partial t}\{48 + 49 + C.C.\}$$

$$= -4\pi\, s n_k \delta_{k_1 k'} \mathrm{Re}\left\{\int\sum s_1 A^{-++}_{k12} C^{+---+}_{k1244} n_2 n_4 \delta(-sk+s_1k_1+s_2k_2)\right.$$
$$\left.\delta(-s\omega+s_1\omega_1+s_2\omega_2)dk_1 dk_2 dk_4\right\} \qquad (4\text{-}8)$$

Diagram 50

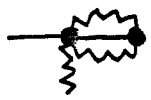

$$= -is \iint \sum \int_0^t C^{-++++}_{k1234}(t') \int_0^{t'} (-is_2) A^{-++}_{256}(t'')dt''dt' \delta(-s_2k_2+5+6)$$

$$\delta(-sk+1+2+3+4)\, n_1 n_3 n_4\, \delta_{1-5}\delta_{3-6}\delta_{4-k'} dk_1 - dk_6$$

$$= -sn_k \delta_{k-k'} \int \sum \int_0^t C^{-++++}_{k123k}(t') \int_0^{t'} s_2 A^{---}_{123}(t'')dt''dt'$$

$$n_1 n_3\, \delta(s_1k_1+2+3)\, dk_1 dk_2 dk_3$$

Note that:

$$\sum_{s_1 s_2 s_3} s_2 C^{-++++}_{kk123}\, A^{---}_{123} = -\sum_{s_1 s_2 s_3} s_2 C^{-+---}_{kk123}\, A^{+++}_{123}$$

$$= -\left(\sum_{s_1 s_2 s_3} s_2 C^{-++++}_{kk123}\, A^{---}_{123} \right)^*$$

$\therefore$

$$\{50\} = -\{50\}^*$$

$$\{50\} + \{50\}^* = 0 \qquad (4\text{-}9)$$

Diagram 51

$$= (-is)\int\int \sum \int_0^t C^{-+++}_{k1234}(t')dt'(-is')\int_0^t A^{-++}_{k'56}(t')dt'$$

$$n_1 n_3 n_4 \delta_{1-2}\delta_{3-5}\delta_{4-6}\,\delta(-sk+1+2+3+4)\,\delta(-s'k'+5+6)dk_1 - dk_6$$

$$= \delta_{k-k'}\int \sum \int_0^t C^{-+-++}_{k1134}(t')dt' \int_0^t A^{+--}_{k34}(t')dt'$$

$$n_1 n_3 n_4\, \delta(sk-3-4)\, dk_1 dk_2 dk_4$$

$$\frac{\partial}{\partial t}\{51\} \propto C^{-+-++}_{k1134}\, A^{+--}_{k34}\left\{ e^{-i(-s\omega+3+4)t}\int_0^t e^{i(-s\omega+3+4)t'}\, dt' \right.$$

$$\left. + e^{i(-s\omega+3+4)}\int_0^t e^{-i(-s\omega+3+4)t'} dt' \right\}$$

$$= 2C^{-+-++}_{k1134}\, A^{+--}_{k34}\left\{ \frac{\sin(-s\omega+3+4)t}{-s\omega+3+4} \right\}$$

$$\therefore \lim_{t\to\infty} \frac{\partial}{\partial t}\{(51) + C.C.\}$$

$$= 4\pi\, \delta_{k-k'} \mathrm{Re} \int \sum C^{-+-++}_{k1134}\, A^{+--}_{k34}\, n_1 n_3 n_4\, \delta(sk-3-4)\,\delta(s\omega-3-4)dk_1 dk_3 dk_4$$

(4-10)

Diagram 52

$$= (-is)\, n_k\, \delta_{k-k'} \int \sum \int_0^t D^{+-+-+-}_{kk1122}(t')dt'\, n_1 n_2 dk_1 dk_2$$

D^{+-+-+-}_{kk1122} is Real

$\Rightarrow$ Term 52 is pure imaginary

$$\therefore \quad \{ 52 + C.C. \} = 0 \tag{4-11}$$

Thus, diagrams 48, 49, and 51, which include effects of the quartic nonlinearities produce a nonzero contribution to the kinetic equation if resonance with three wave numbers ia allowed (4-5). The quintic term, diagram 52, does not contribute at this order.

5. DISCUSSION

Starting with a general Hamiltonian description of a wave field, and including terms up to order (amplitude)^5, a consistent perturbation expansion has been obtained. By including quintic nonlinearities in the equations of motion, the kinetic equation is accurate up to terms of order (amplitude)^6.

Most authors have restricted their attention to quadratic nonlinearities, although the leading term in the kinetic equation (order ε^4) will formally include a contribution from the cubic nonlinearity (diagram 4). We have shown that this term cancels out, and the order ε^4 term in the kinetic equation is accurately described by quadratic interactions. If resonance among three wave numbers is not possible, the dominant term in the kinetic equation is of order ε^6, and the neglect of higher order nonlinearities is inconsistent.

At least one author (Hasselman 1966) has considered a general expansion of the Hamiltonian. The results given here include nonzero terms not obtained by that analysis. It has been shown that diagrams 48, 49, and 51, corresponding to quartic nonlinearities produce nonzero contributions to the kinetic equation at order ε^6. Since Hasselmann has not presented the details of his analysis, it is unclear where these terms are lost.

We have shown that the quintic terms (diagram 52), although formally of order ε^6, do not contribute to the kinetic equation at this order.

For practical applications, one only retains the first non-vanishing terms in the kinetic equation. If resonance with three wave numbers is possible, the leading order contribution comes from the quadratic nonlinearity in the equations of motion. The cubic and quartic terms do contribute, but they are of higher order.

If resonance with three waves is excluded by the dispersion relation, the spectral energy flux is of order ε^6. In this case, the extra diagrams 48, 49, and 51 do not contribute to the energy flux on a time scale long compared to the period of the basic oscillation.

Whether or not resonance occurs with three wave numbers, the leading order terms in the kinetic equation are not affected by quartic or higher order nonlinearities. For the case of resonance with three waves, only the quadratic nonlinearity enters into the kinetic equation. If this resonance is excluded, it is sufficient to include only the quadratic and cubic terms to obtain the kinetic equation to leading order (ε^6). The quartic and quintic terms, although formally producing terms of order ε^6, do not contribute in this case.

REFERENCES

D. J. Benney and P. G. Saffman, Nonlinear Interactions of Random Waves in a Dispersive Medium, Proc. Roy. Soc. A 284 (1966), pp. 301-320

K. Hasselmann, Nonlinear Interactions Treated by the Methods of Theoretical Physics, Proc. Roy. Soc. A 299 (1967), pp. 77-100

_____, Feynman Diagrams and Interaction Rules of Wave - Wave Scattering Processes, Rev. Geophys. 4 (1966), pp. 1-32

O. M. Phillips, On the Dynamics of Unsteady Gravity Waves of Finite Amplitude, J. Fluid Mech. 9 (1960), pp. 193-217

H. W. Wyld, Jr., Formulation of the Theory of Turbulence in an Incompressible Fluid, Ann. of Physics, 14 (1961), pp. 143-165

V. E. Zakharov, Weak Turbulence Spectrum in a Plasma Without a Magnetic Field, Sov. Phys. JETP 24 (1967) pp. 455-459

_____, Stability of Periodic Waves of Finite Amplitude on the Surface of a Deep Fluid, J. App. Mech. and Tech. Phys. 9 (1968), pp. 86-94

_____, The Hamiltonian Formalism for Waves in Nonlinear Media Having Dispersion, Radiophysics and Quantum Electronics 17 (1974), pp. 326-343

V. E. Zakharov, V. S. L'vov, and S. S. Starobinets, Instability of Monochromatic Spin Waves, Sov. Phys.-Solid State 11 (1970), pp. 2368-2373

V. E. Zakharov and V. S. L'vov, Statistical Description of Nonlinear Wave Fields, Sov. Phys.-Radiophysics 18 (1974) pp. 1084-1097